53-1-6

APGC-TDR-62-69

Terminal Ballistic Investigation of the Impact and Effect of Ultra High Speed Micron-Size Particles Produced on Hypervelocity Impact

APGC Technical Documentary Report No. APGC-TDR-62-69

NOVEMBER 1962 • AFSC Project No. 5841

DEPUTY FOR AEROSPACE SYSTEMS TEST

AIR PROVING GROUND CENTER

AIR FORCE SYSTEMS COMMAND • UNITED STATES AIR FORCE

EGLIN AIR FORCE BASE, FLORIDA

(Prepared under Contract No. AF 08(635)-2099 by Utah Research and Development Co., Salt Lake City, Utah)

291822

FOREWORD

This is the final report of a program conducted under Air Force Contract No. AF 08(635)-2099, "Terminal Ballistic Investigation of the Impact and Effect of Ultra High Speed Micron-Sized Particles Produced on Hypervelocity Impact." Project Director at Utah Research and Development Company was Dr. Emerson T. Cannon. Mr. Andrew Bilek of the Ballistics Branch, Directorate for Aerospace, was the Project Manager.

Catalog cards may be found in the back of this document.

ABSTRACT

This TDR reports the results of the investigations of spray particle impact. A method was devised to measure the velocity and calculate the diameter of the spray particle in flight. The crater produced at impact was measured to obtain the diameter and several attempts to measure penetration and volume are described. A scaling law relating macro size craters to micro craters produced at the same velocity is presented.

PUBLICATION REVIEW

This technical documentary report has been reviewed and is approved.

Morrill E. Marston

MORRILL E. MARSTON
Colonel, USAF
Deputy for Aerospace Systems Test

CONTENTS

LIST OF ILLUSTRATIONS

SUMMARY

When a pellet strikes a target, tiny secondary projectiles are ejected. These spray particles have been measured to have velocities of 10 km/sec and higher. They are luminous; and when they impact on a secondary target, their microscopic craters have the appearance and shape of normal macrocraters. The spray particles were used to study hypervelocity impact.

These studies of microcraters led to the following conclusions:

1. The crater parameter which can be measured in both the micro and macro scale is the crater diameter.

2. When the crater diameter is normalized by the particle diameter and plotted against velocity at impact, the resulting curve is common to macro and micro particle impacts.

3. Micro effects may be predicted from macro particle impacts because the ratio of the crater diameter to pellet diameter is independent of pellet diameter.

4. Spray particles are extremely difficult to use as tools for impact studies but may be used for trail and ionization studies.

1. INTRODUCTION

This project was first conceived at Utah Research and Development Company as an attempt to discover a means by which discrete particles could be accelerated to velocities approaching meteoroid velocities. The scientific and engineering benefits which would come from studying laboratory controlled simulated meteoroids are numerous. The literature at that time, 1960, contained no report of success in accelerating particles above 15,000 fps in controlled situations. It seemed natural to seek for some method which would produce particles whose velocities were high, up to 50,000 fps and whose dimensions and composition were known.

While studying at the University of Utah and following research at the University of Utah High Velocity Laboratory, Dr. William H. Clark and Thomas W. Lee, both now of URDC, became interested in the "star" associated with an ordinary high velocity metal-to-metal impact. Open-shutter photographs of impacts showed that the streaks of light coming from the point of impact were stopped when an obstruction was placed in their path. Moreover, there was a flash at the secondary impact. Preliminary investigations into the nature of the particles with which the light streaks and the secondary impact flashes were associated showed that they were microparticles whose velocities were on the order of 10 km/sec. The primary impact ejecting this spray was only on the order of 2 km/sec.

This increase in velocity suggested that the spray particles could be used as a tool for studying hypervelocity phenomena. Projectiles moving at this velocity leave a luminous trail that is similar to the trail behind a meteor. If a single spray particle could be isolated, whose velocity were known, it was postulated that much could be learned in the laboratory regarding trail physics. It was also noted that the material of the spray particle could be varied at will to simulate warheads in a re-entry situation for a military application.

The secondary impact or the impact of the spray particles on a secondary target also attracted attention. Upon microscopic examination, it was seen that the secondary target contained beautifully formed typical hypervelocity craters.

More preliminary work led the investigators to believe that it was now entirely possible to create artificial micrometeoroids in the laboratory and to use them as a tool to study the physics of their trails and the physics of hypervelocity impact in the velocity range from 9 km/sec up.

Utah Research and Development Company formally proposed to study the ionization in the trails of the spray particles in order to understand the physics of meteor trails. URDC proposed also to study the craters produced by microparticles at these extreme velocities for two reasons: to understand the physics of impact; and to produce engineering data whereby damage to satellites and missiles could be predicted. A third portion of the proposal was to study the possibility of a scaling law which would predict macroparticle impact characteristics from microparticle impact parameters.

The research contract was awarded by the Air Force with slightly modified goals. The task as outlined by the contract was to study the cratering effect of micron-size particles whose impacting velocities would be up to 50,000 fps, and to obtain from the above craters a relationship for the volume of the crater versus the energy required to produce it; a relationship for the ratio of particle penetration to particle diameter versus velocity; and a relationship that would show the existence or non-existence of a scaling law to go from micro to macro scale. It was suggested that some trail physics study be undertaken but that at least 85% of the effort be expended in the study of terminal effects.

2. RESEARCH PROGRAM

The experimental investigation under this contract followed three main phases. First, it was important to know the velocity of the spray particle as it traversed the spray particle range. Second, it was necessary to know as much as possible about the crater formed by the spray particle as it impacted on the secondary target. Third, it was desirable to obtain the maximum velocity spray particles possible. The investigations followed these main lines of exploration.

All of the basic equipment to do this research was in existence at Utah Research and Development Company at the beginning of the contract. It was only necessary to purchase one oscilloscope and modify some of the existent hypervelocity ranges.

The measurement of the velocity of the spray particles required some specialized techniques that were difficult to perfect. The various approaches to this problem will be discussed in following sections. The need for the highest possible impact velocity spurred one phase of this investigation. Higher velocity in the secondary particle was sought by increasing the velocity of the primary particle. It was also suspected that higher velocity would come from reducing the mass of the secondary particle. Thirdly, it was hoped that higher velocities could be discovered in an optimum exit angle from the primary impact.

Several approaches were made to the problem of the crater. Since the craters were all microscopic, techniques to measure crater parameters in the 10^{-3} - 10^{-4} cm range had to be developed. These approaches and their results are discussed in following sections.

3. RESEARCH FACILITIES

3.1 Guns

Two types of launchers were used to shoot the primary projectile in this research program. The first type was a simple smooth-bore powder gun. The second type was the URDC light-gas gun. The powder gun used for most of the shots of this investigation was a 1/4" bore gun 5' long. It was chambered for a .243 cartridge and is fired remotely by closing a circuit which energizes a solenoid. The plunger in the solenoid drives into the firing pin which fires the shell. This simple gun proved to be very effective and reliable.

A standard powder load was agreed upon early in the program. The shell was loaded with 1 cc of DuPont #4064 rifle powder, then the remainder of the cartridge was filled with Hercules #2400 powder. The 1/4" steel sphere was then forced into the mouth of the shell. This load was so reliable that for the more than 200 shots whose primary velocity was measured, it was shown that the velocity was invariably 2.2 ± 0.01 km/sec.

The powder gun was also exceptionally accurate. On various occasions checks were made to test the accuracy of the gun. The most critical test was to shoot two or more shots without changing the target. The powder gun accurately shot each succeeding shot into the bottom of the previous crater.

The gun was rigidly clamped into position as shown in Figure 1. Later more rigid clamps were used as seen in Figure 2; but for the powder gun the earlier wires were satisfactory.

The light-gas gun used in later phases of this project is seen pictured in Figure 3 and diagrammed in Figure 4. The gun has a 20' long pump tube and a 48" launch tube. The inside bore of the pump tube is 1"; the bore of the launch tube is 1/4". The light gas used at URDC is exclusively hydrogen.

The gun is a simple two-stage launcher. The powder charge (See Figure 5) is ignited. The expanding powder gases drive the plastic

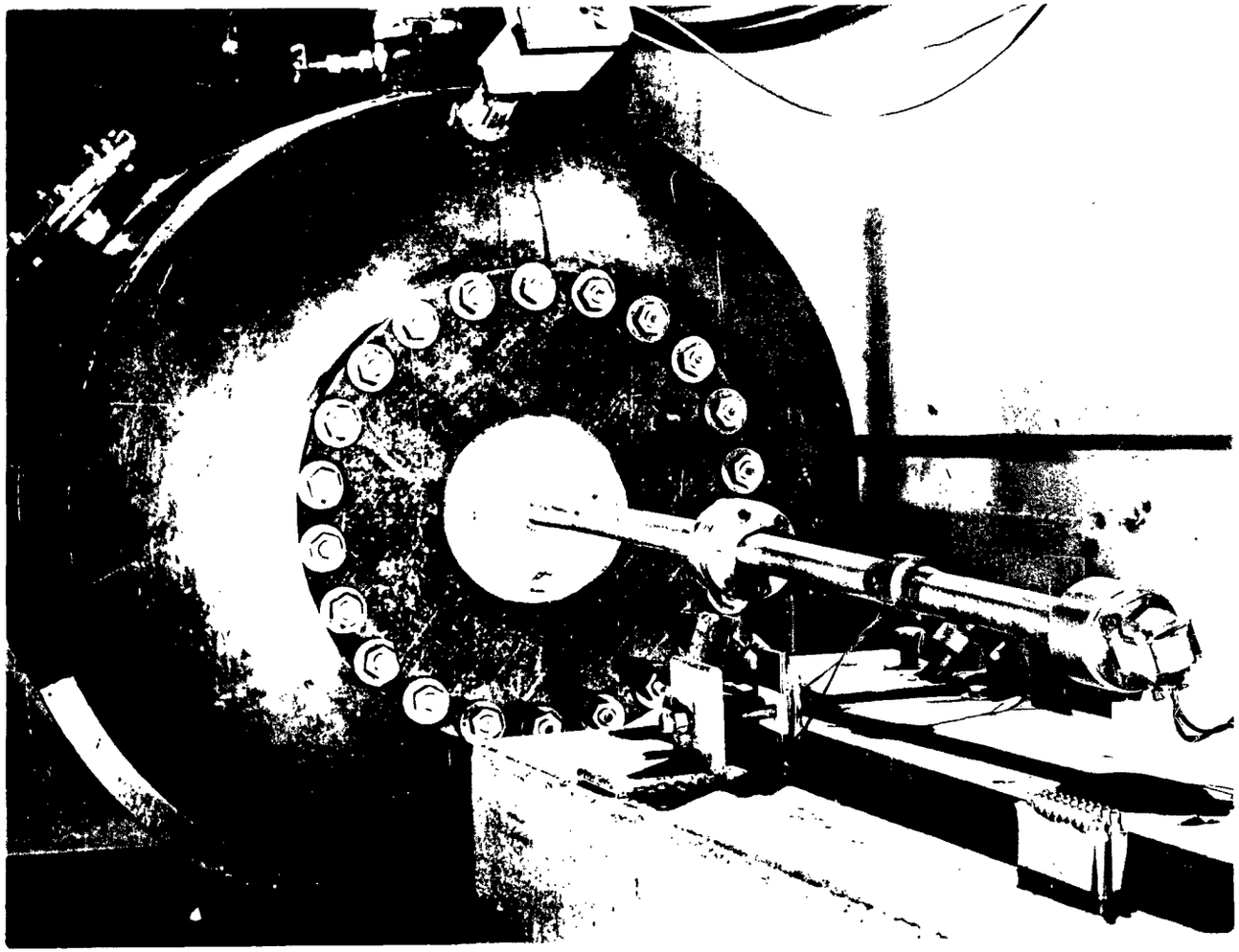

Figure 1 - Powder Gun and Tank (Wired)

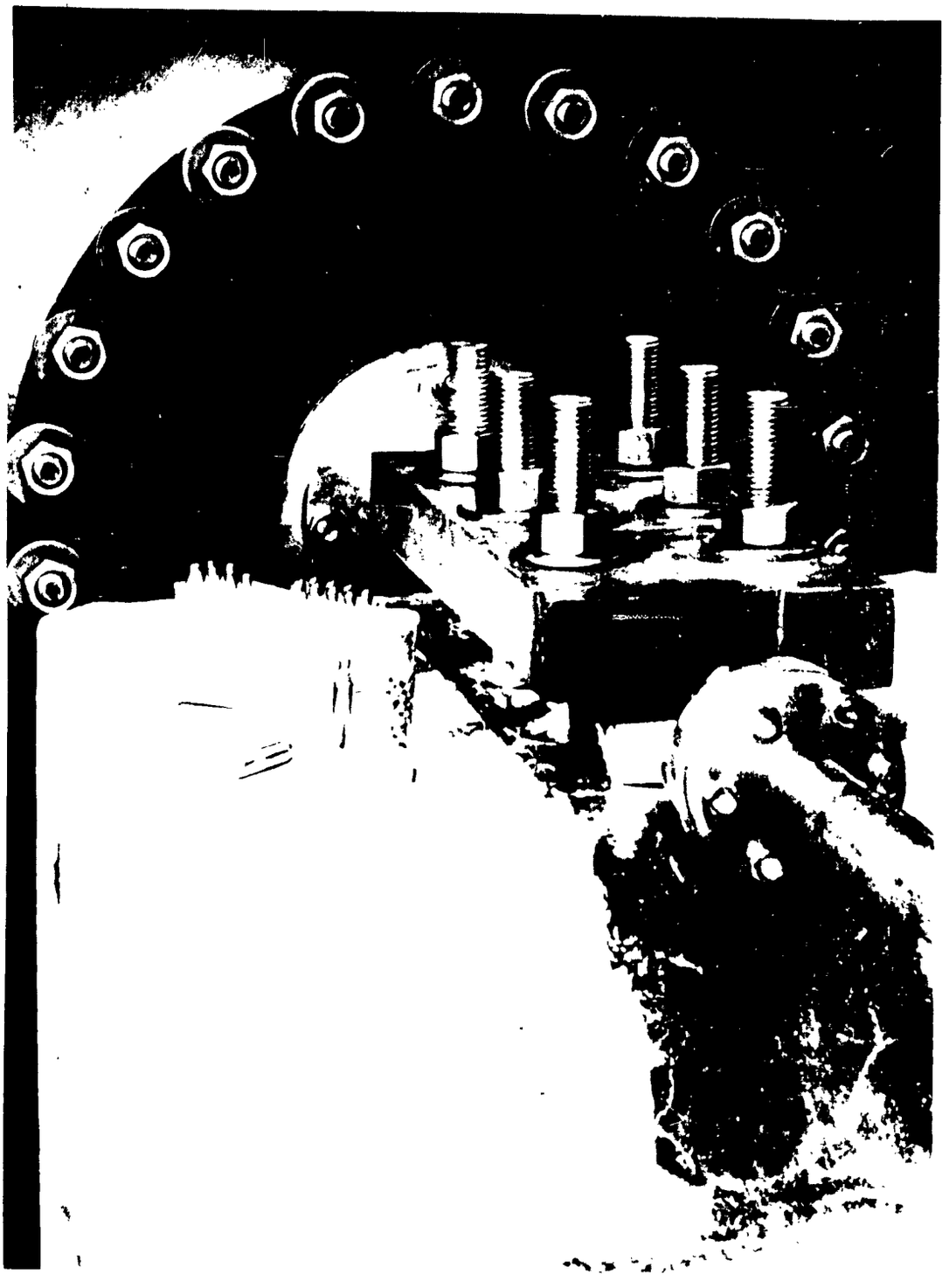

Figure 2 - Rigid Clamp on Powder Gun

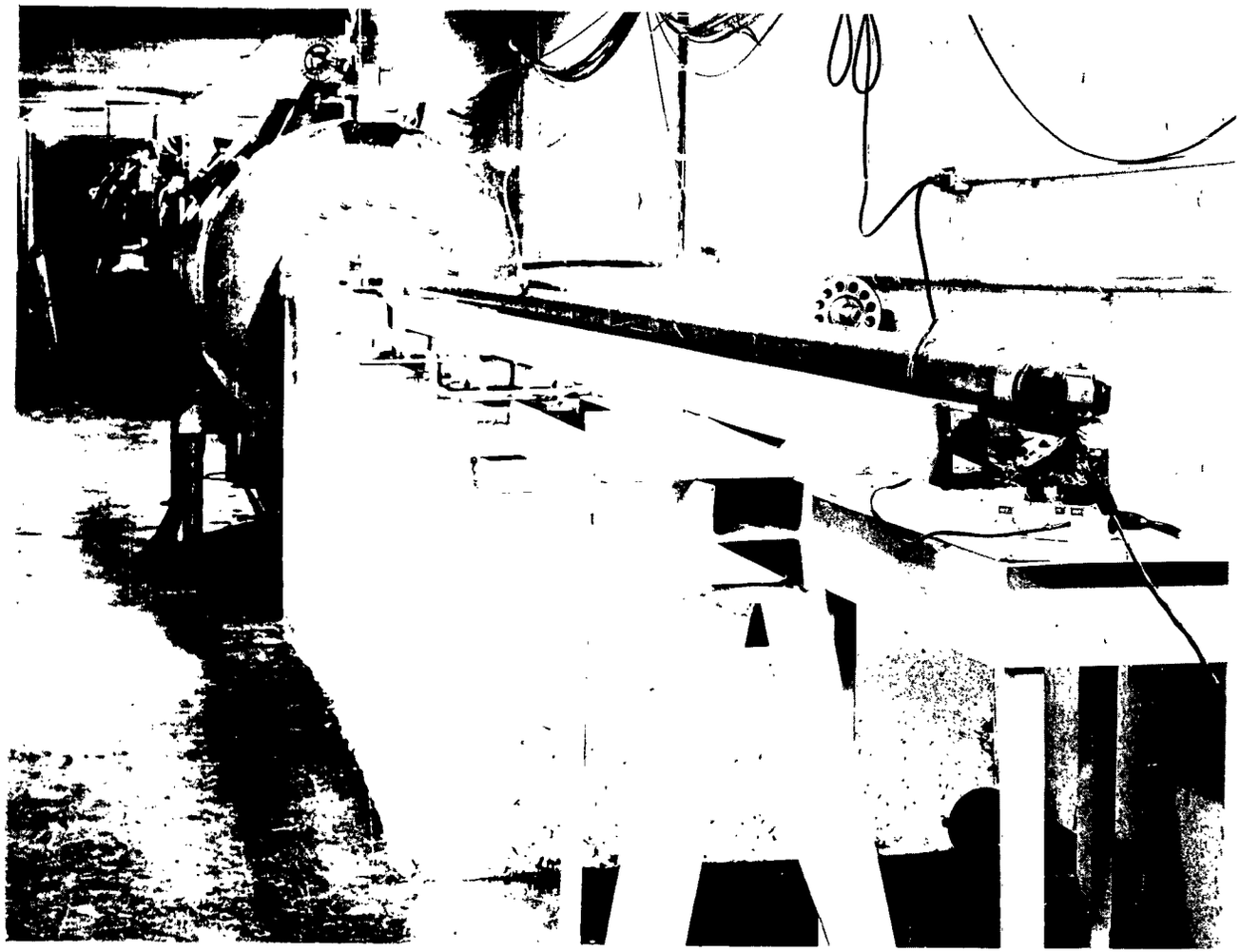

Figure 3 - URDC Light-Gas Gun

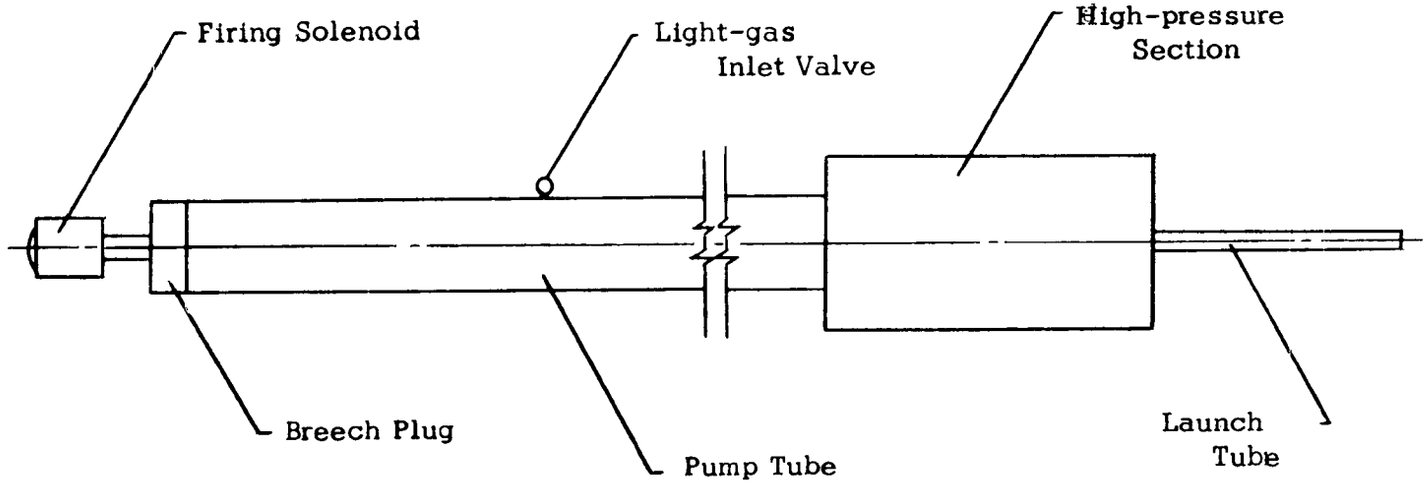

Figure 4
URDC Light-gas Gun

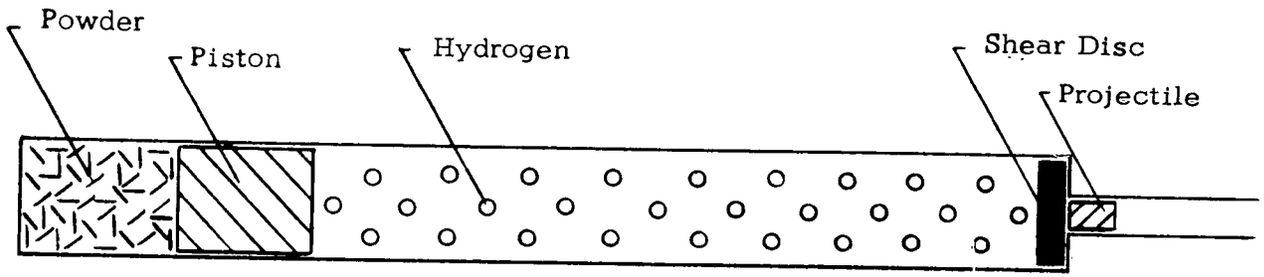

BEFORE FIRING

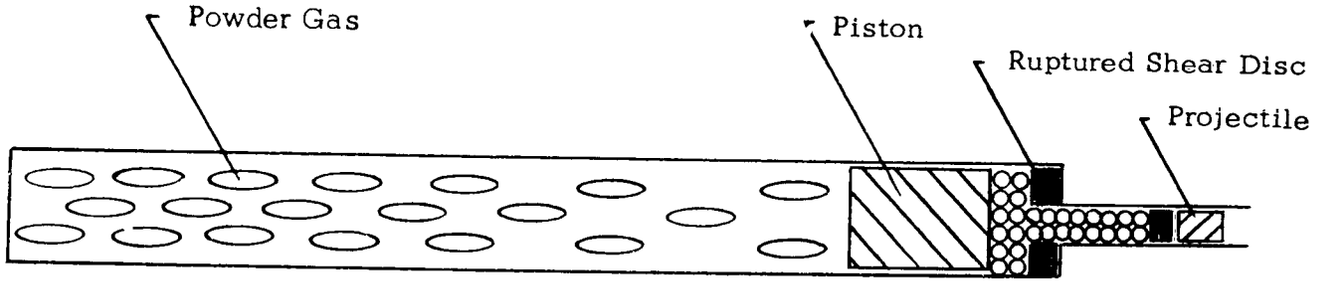

DURING FIRING

Figure 5

Light-gas Gun Schematic

piston down the pump tube compressing the hydrogen gas in front of it. As the gas is compressed and the pressure builds, the point is reached where the shear disc fails and the gas begins to expand down the launch tube, pushing the pellet in its sabot ahead of it. The gas pressure continues to build behind the sabot in the high-pressure section of the pump tube. The hot high-pressure hydrogen follows down the launch tube and accelerates the projectile.

There are several unknown factors in the operation of a light-gas gun which tend to reduce both the accuracy and the repeatability of the gun from shot to shot. Much work was done to overcome these difficulties because accuracy is extremely important in this work as will be seen when the spray particle range is discussed. Some improvement in accuracy was achieved by improving the gun mount and by constructing a solid, rigid, massive clamp for the launch tube. The impact circle was reduced from more than 12 inches to less than 5 inches. Unfortunately even this improvement was not sufficient to be completely satisfactory for spray particle work. The light-gas gun is capable of a maximum muzzle velocity of something over 6 km/sec. The light-gas gun also tends to show wide variations in velocity even though all gun parameters (the powder load, the piston size and weight, the H_2 charge, the shear disc, the pellet, and the sabot size and weight) are held constant. No sure explanations have been found for this wide variation in velocity. Understandably, a good deal of effort has gone into controlling the muzzle velocity as well as trying to increase the maximum attainable velocity.

3.2 Primary Pellet Ranges

Two vacuum ranges were used in this investigation. Both were already in existence at the beginning of this project. Both ranges can accommodate both the powder gun and the light-gas gun though the second range is less satisfactory than the first for use with the light-gas gun because the accuracy requirements are much more stringent in the second range.

The first range is seen pictured in Figure 6 and diagrammed in Figure 7. This range was constructed to physically separate by

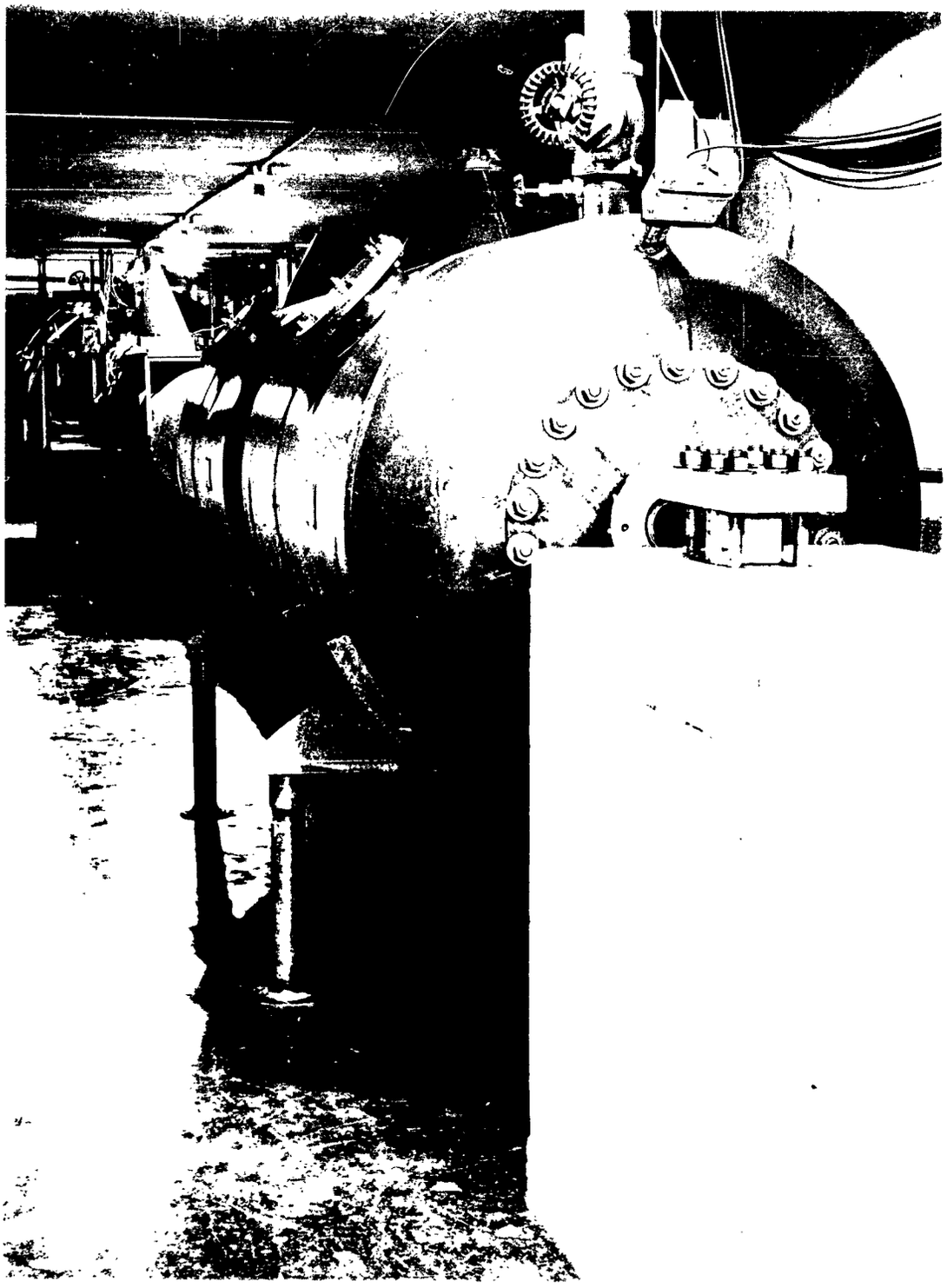

Figure 6 - First High Velocity Range

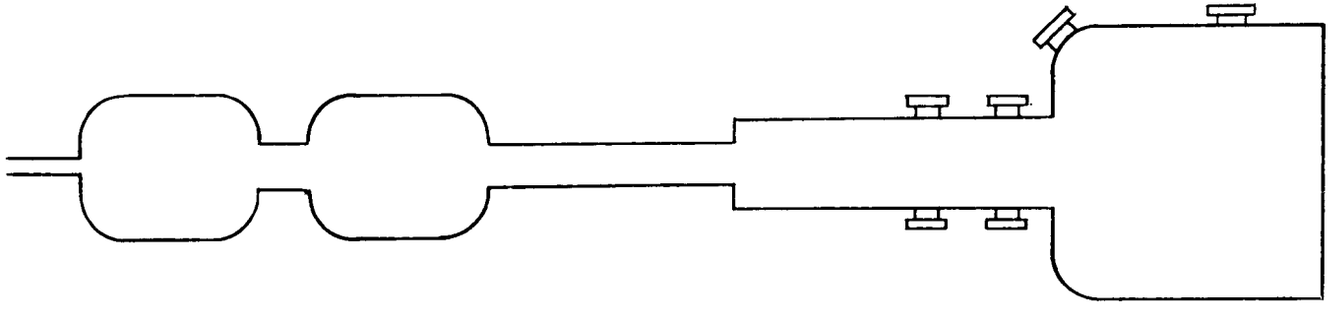

Figure 7

Range in Tunnel 6 (Without Baffles)

distance the impact area from the muzzle blast of the gun. It is more than 15 meters from the muzzle to the primary target.

The major portion of the hot hydrogen is trapped in the two eight-foot blast tanks. Each of these tanks is four feet in diameter and eight feet long. They are separated by a wall which has a five-inch hole in the center. This baffle plate or wall effectively screens off the greater portion of the blast. The gas that gets through the hole is allowed to expand into the second baffle tank where more of the remaining gas is trapped. The residual tank pressure effectively slows down the remaining hot hydrogen following the primary projectile while not significantly affecting the velocity of the heavier metal sphere.

The ultimate vacuum obtainable in the large range is just 6 mm of mercury. There are several reasons for this poor vacuum. The seal on the massive back door is imperfect and after several years of shooting into this tank some seams have opened up. No real effort has been made to achieve a better vacuum because for the work in this range 6 mm of mercury pressure is very satisfactory. Any work that requires pressures below this pressure can be, and is, done in the second vacuum range.

The second vacuum range is seen pictured in Figure 3 and is sketched diagrammatically in Figure 8. As is seen in the diagram, not only is the total volume of the tank smaller than the first range, it is also more elaborately baffled. Also, every seal is either welded to a high-vacuum seal or fitted with O-rings. In addition, there is associated with this range, both a roughing vacuum pump and a diffusion pump. The ultimate pressure in this tank is in the 10^{-4} mm of mercury range.

The baffling is a series of steel cones welded inside the tanks. At the apex of each cone there is a one-inch hole. At these extremely low tank pressures there is not the residual atmosphere to slow down the trailing muzzle blast so it must be shaved away by the baffles. Figure 8 shows the actual number and distribution of the baffles. It will be noted that the first baffle is a flat plate with a one-inch hole cut in the center rather than a cone. This was done because it was convenient to weld the baffles to existing supports already within the tanks. A cone at the first support point would not have fit in the tank. These

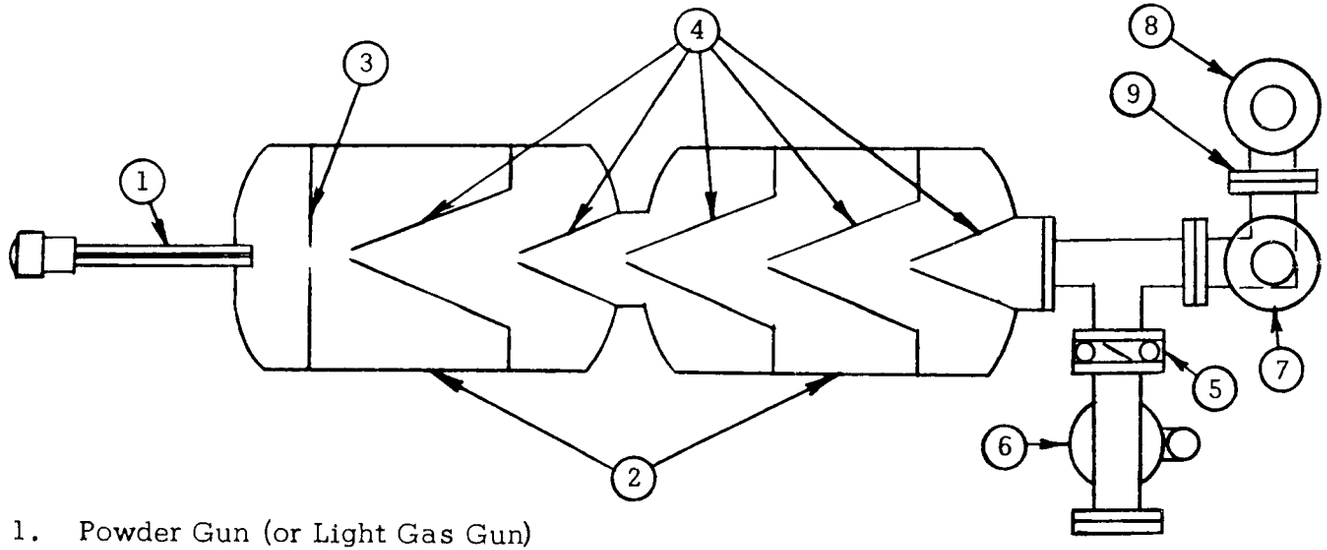

1. Powder Gun (or Light Gas Gun)
2. Vacuum Tanks
3. 1st Baffle
4. Baffles (cones)
5. Vacuum Range
6. Diffusion Pump
7. Primary Target Assembly
8. Secondary Target Assembly
9. Any length Spray Particle Range may be inserted here.

Figure 8. Tunnel Vacuum Range

baffles satisfactorily shield the primary target area so that the muzzle blast not only does not interfere with any experiment at the impact area, the pressure does not rise until well after the impact.

3.3 Spray Particle Ranges

The original spray particle range was mounted on the massive back door of the first vacuum range. It was designed for two purposes. First, it was planned to allow one, or at most just a few, spray particles into the range from the primary impact. Second, it was designed to allow a study of the angular distribution of spray particles. Once the spray particle was isolated, various measurements could be made on it. A picture of the range is seen in Figure 9. The primary target is seen below the metal box. The spray particle passes into the metal box through a very small aperture. Within the box are seen three slits in front of which the spray particle passes. At the top is seen the secondary target holder. It is on the secondary target that the spray particle impacts and forms a microscopic crater.

The entrance aperture to the spray particle range is a long slot about 2 1/2 inches long and 1/4 inch wide. This slot may be masked off so as to use any portion of it that may be chosen. For most of the shots the entrance aperture was chosen to be about 0.3 mm x 0.1 mm and was placed so that one end of the slit was exactly at plane made by the face of the primary target. It had been previously discovered the spray particles traveled in straight lines and that the smallest or microscopic particles were ejected at right angles to the line of flight of the primary pellet. It was suspected that the highest velocity particles would be the smallest. The entrance aperture was adjusted to allow only one spray particle or at worst very few spray particles into the spray particle range each shot.

The additional feature of having the long slot is that the entrance aperture can be moved along the slot to study spray particle velocity and size as a function of exit angle from the plane of the impact or the whole slot could be opened to allow gross measurements of crater size and number distribution also as a function of angle from the face of target.

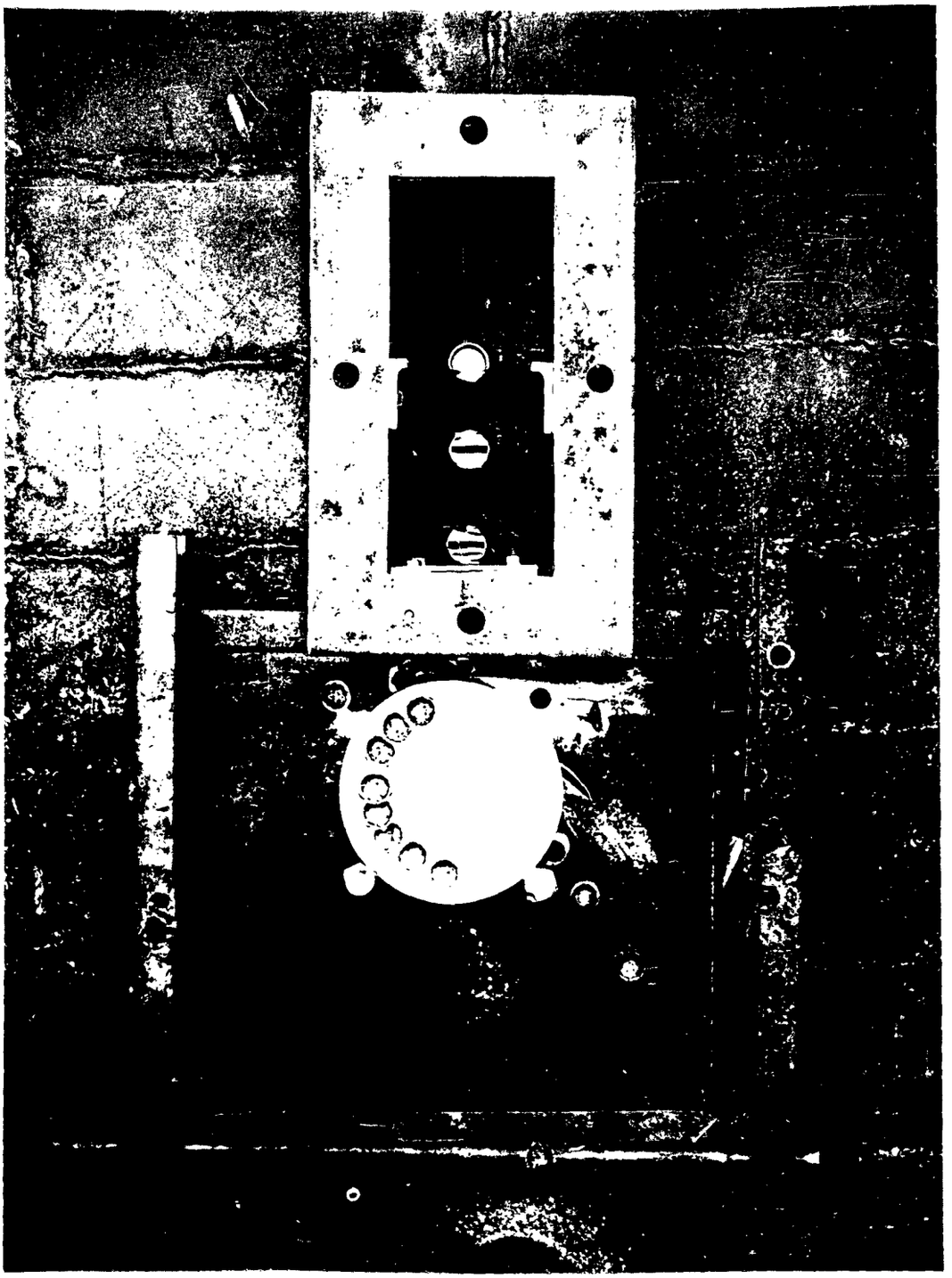

Figure 9 - First Spray Particle Range

The spray particle range in the second installation was designed to measure the drag on spray particles in a highly evacuated situation. The pressure in the first range was 6 mm of mercury whereas the pressure in the second range could go as low as 10^{-4} mm of mercury. In order then to be able to see any drag on a spray particle, it would be necessary to have a much longer range. The path length for the spray particle from impact to secondary target in the first range is 19.6 cm. The spray particle path length in the second range can be anything from 40 cm to more than a meter.

Figures 10a to 10d show the various components of the second spray particle range. Since the distances are longer, specifically the distance from primary impact to entrance aperture of the spray particle range, the dimensions of the entrance aperture can also be larger. The aperture most often used was the 1/4 inch hole shown, though a face plate with any size hole could be substituted for that one. The second most used aperture was 1/8 inch hole.

Figure 10c shows one portion of the new spray particle range. This is the "expandable" section. If a longer or shorter range is desired this section may be replaced with another section of the required length. Within the section can be seen the ends of the light pipes and the slits. It is through these slits that the passing spray particles are observed by the photomultiphers.

In Figures 11a to 11c is seen the secondary target assembly. The assembly is so constructed that the secondary target can be inserted and removed quickly and can be returned to its original location in the assembly accurately. The secondary target is the shiny one inch disc in the picture. The most used distance from primary impact to secondary target in this range was 81 cm.

The secondary target holder was machined to just fit the stage of microscope. It was so constructed that it could be returned accurately to place there and once the settings for a crater are found, it is possible to return the microscope to the settings and re-locate the craters.

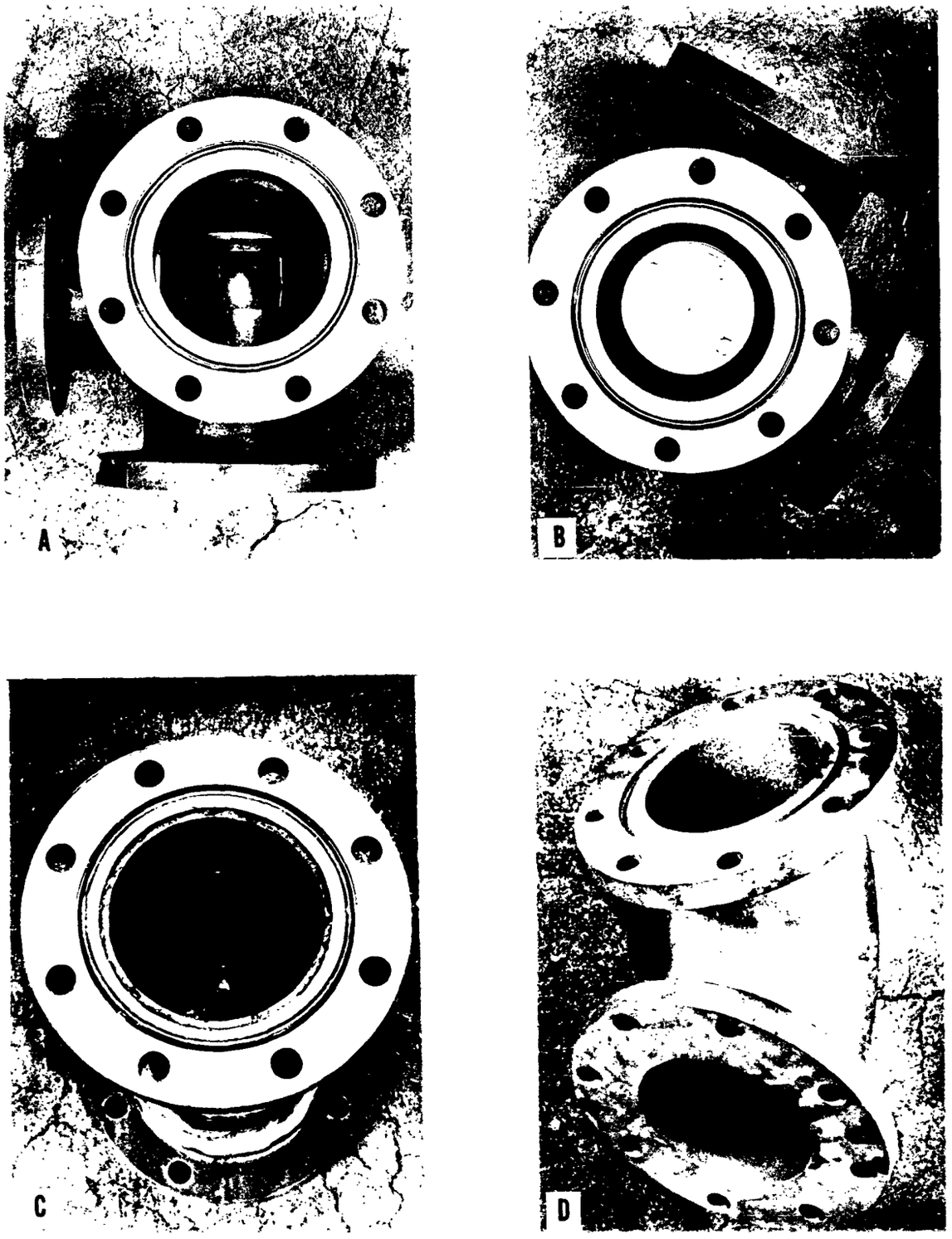

Figure 10 - Second Spray Particle Range

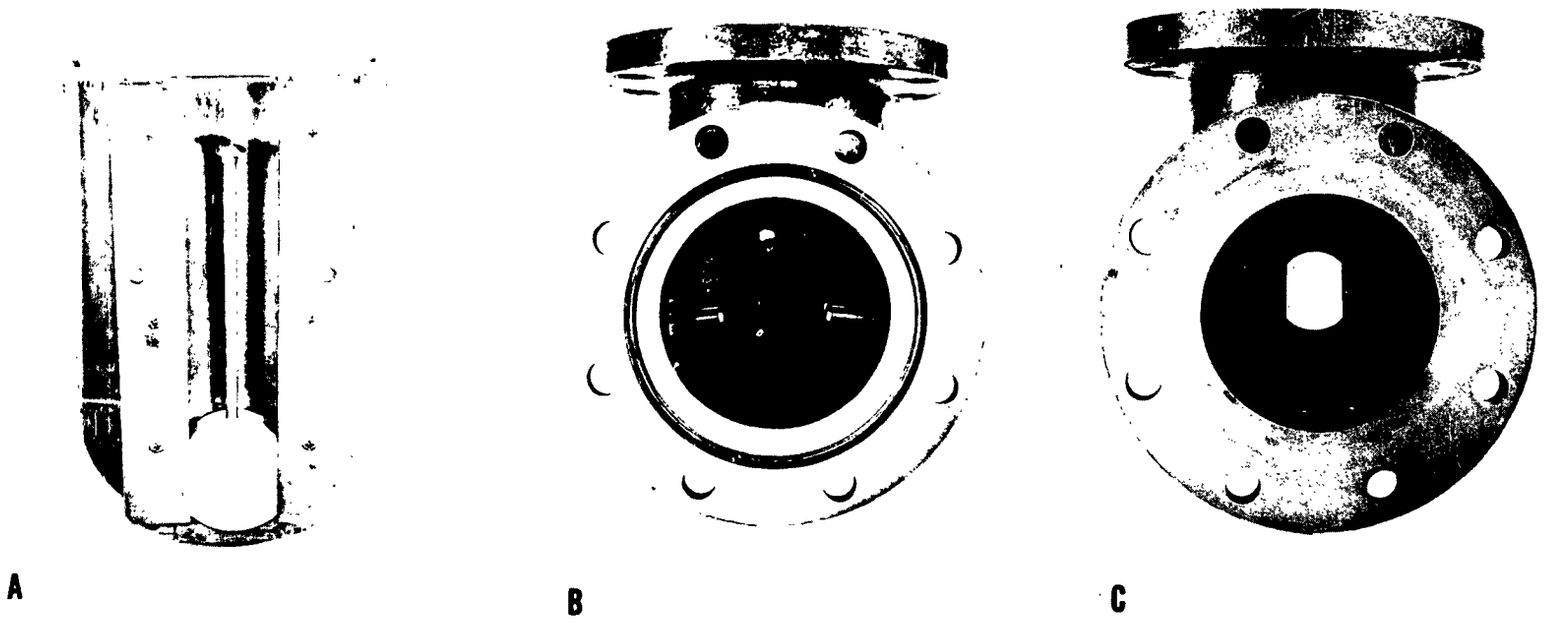

Figure 11 - Secondary Target Assembly

3.4 Primary Velocity Systems

The method used to measure the velocity of the primary projectile in both ranges is the same. In each case a photocell is so positioned that it can see the muzzle flash of the gun. The output of the photocell is amplified and fed into the trigger circuit of an oscilloscope. The oscilloscope has a calibrated sweep rate which accurately measures the passage of time. The sweep is begun by the muzzle flash.

At the target a photocell is positioned to see the impact flash. The output of this photocell is fed into the verticle amplifier circuit of the oscilloscope and there is an abrupt rise in the trace at the distance from muzzle to target by the observed time between the beginning of the trace and break in the trace at impact.

For measuring the velocity from a powder gun the above described system is quite sufficient because the only object flying in the range is the projectile. However, when the light-gas gun is used, there can be a question as to what arrives at the target first. In addition to the steel or aluminum pellet, there are pieces of the sabot and the punched-out portion of the shear disc. To be sure the photocell was seeing the flash from the impact of the metal sphere and not the somewhat smaller and less dense trailing material, an accelerometer was mounted on the target support behind the target. The accelerometer distinguishes very well the difference between a heavy mass impact and light mass impact. The output of the accelerometer was fed onto the verticle amplifiers of a second trace of the same oscilloscope. When the breaks on the two parallel traces coincided there could be no question as to the velocity of the pellet.

3.5 Spray Particle Velocity Systems

The method used to measure the time required for the spray particle to traverse the spray particle range was similar in both ranges. Each range has three observation ports which view the path which the spray particle follows. At each port is a photomultiplier. The output of each photomultiplier is presented on the trace of an oscilloscope which was triggered by the primary impact flash. The

trace is photographed and the time is measured from the oscilloscope trace. The time measured at each port is the total transit time and the velocities calculated from these times and the known distances are only average velocities. The instantaneous initial velocity and the velocity at spray particle impact must be calculated from the drag equations which will be discussed in a succeeding section.

In order to locate the spray particle more accurately in space while measuring its time of transit, it was necessary to collimate the light available to the photomultipliers. This was done by extending light pipes from the windows out to near the path of the particle. A narrow slit mask was then placed over the end of the pipe. Only when the luminous particle was directly in front of the slit was it possible for the photomultiplier to see it. The distance to each slit from the primary impact was carefully measured. The final light pipe was masked so the photomultiplier could see the impact flash of the spray particle on the secondary target.

The distances in the first range were fixed and could not be changed. The entrance aperture was 7.7 cm from the primary impact. The first photomultiplier slit was at 10 cm and the second photomultiplier slit was at 15 cm. The secondary target was 19.6 cm from the point of primary impact. The new range is more flexible in that all of the lengths beyond the entrance aperture to the spray particle range the length of the range could be varied quite a bit. The range section pictured in Figure 10c had the first photomultiplier at 35 cm the second at 55 cm and the secondary target at 81 cm.

During the shot the velocity of the primary projectile is measured and the arrival time of the spray particle at each photomultiplier station is recorded. From this data the size of the spray particle and its impact velocity are calculated. It is then necessary to make measurements on the results of that impact, the crater. The crater from a typical spray particle impact is from 5 - 50 microns in diameter.

3.6 Secondary Target

The secondary target is a circle 2.5 cm in diameter. It is frequently difficult to find and identify the crater. The secondary

target aluminum was 2024T4. When this grade aluminum is subjected to hypervelocity impact on the macro-scale, the lips of the forming crater are brittle and break off. On the micro-scale the crater lips form beautifully just like they do in lead at lower velocity on the macro-scale. Each crater is circular, (See Figure 12); deep in the center, and the petals curl out and glisten under the illumination for the microscope.

3.7 Metalograph Microscope

The tool used to search for and measure the diameters of the spray particle craters was a stero eyepiece metalographic microscope. The microscope stage has a 2.5 cm travel in each direction so it was possible to scan the entire secondary target if necessary. The eyepiece is fitted with a scale which gives a known number of microns per scale division for each microscope objective used. Once the crater was located, it was immediately possible to measure its diameter and if so desired photograph the crater for later inspection.

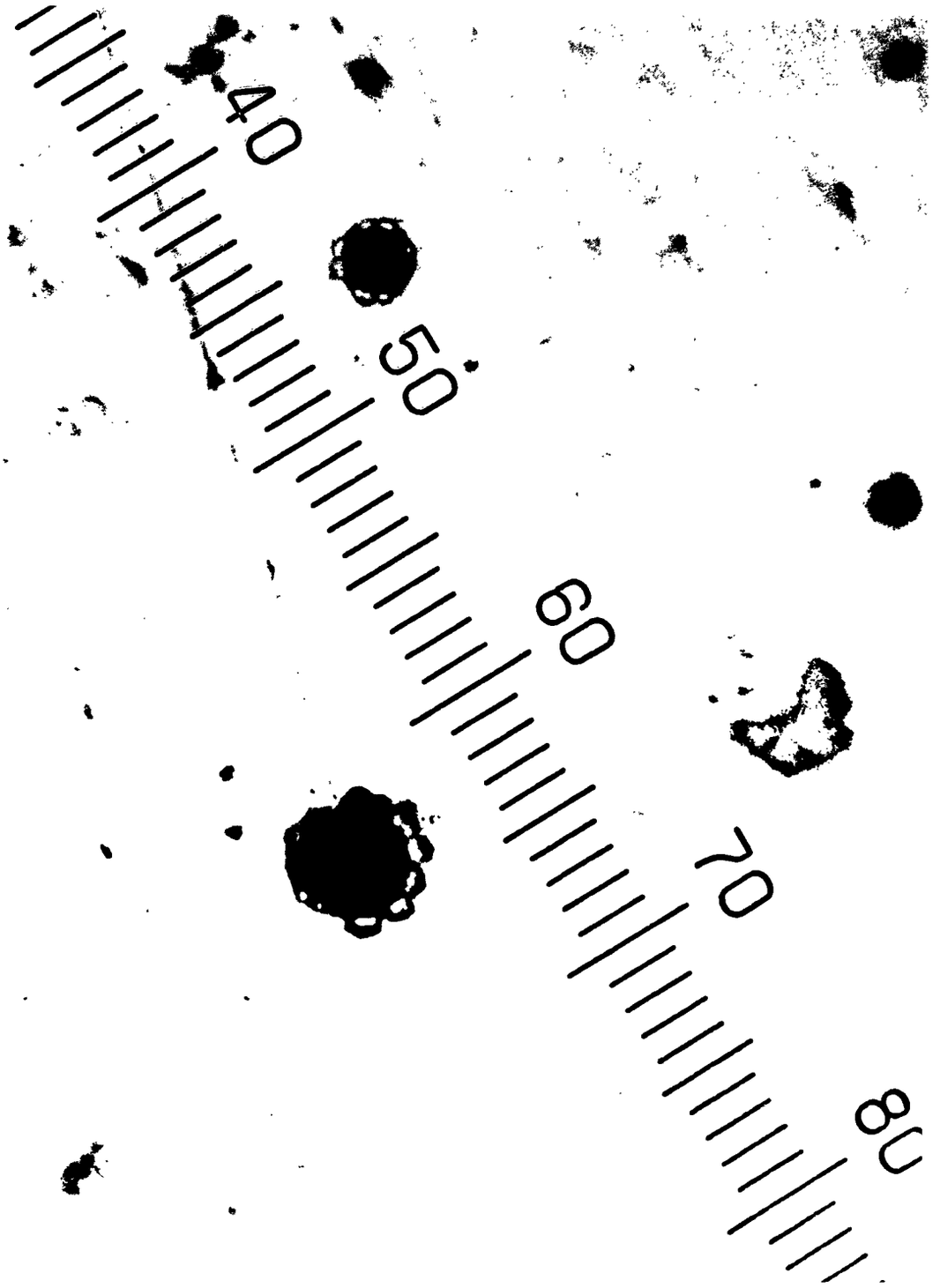

Figure 12 - Secondary Particle Crater

4. THEORY

The size of the spray particles are not, of course, known before the shot nor can the particles be captured and measured because they are destroyed upon impact on the secondary target, and there is some mass lost as they traverse the range. It is necessary therefore to make some measurements during the flight of the spray particle which can be related to the size of the particle and from which the physical dimensions can be calculated. In this work the spray particle diameters have been determined from the rate at which these particles lose velocity. The smaller the spray particle, the more rapidly it will slow down from friction with the atmosphere. The rate of loss of velocity was measured by the experimental techniques described before.

4.1 Spray Particle Shape

The spray particle gives up its energy by interacting with the atmosphere. Air molecule collisions with fast metal objects are not perfectly elastic. Some energy appears as heat in the metal. What fraction this heat is of the total energy involved per collision is not at present accurately known. Rough calculations, however, indicate that spray particles having an initial velocity of around 10 km/sec are melted quickly. Although some mass is lost in flight due to evaporation off the surface, the diameter of the particle is not seriously changed.

The spray particles which either leave the primary impact as liquid droplets or melt in a very short path length are then accurately spherical in shape.

Öpik [1] in his treatise points out that a liquid droplet will be spherical when the radius meets the requirement.

$$r_s \leq \frac{4S}{P_s}$$

where

r_s = radius of sphere

S = surface tension = 1500 dynes/cm

P_s = drag/unit area = $k\rho v^2$

k = 1 in case of small particle and no air cap

Consider the case of a particle whose velocity is 10 km/sec traveling in an atmosphere of 6 mm of Hg pressure. The maximum radius for a stable sphere would be

$$r_s = \frac{6 \times 10^3}{10^7} = 6 \times 10^{-4} = 6 \text{ microns}$$

When the diameter of the sphere is on the order of 10 microns or less, the sphere is stable and unflattened by drag forces. The spray particle diameters measured were mostly on the order of 5 microns and well within the stable limits.

4.2 Spray Particle Diameter

In differential equations the rate at which a spray particle decelerates is

$$\frac{d^2 v}{dt^2} = k \left(\frac{dx}{dt}\right)^2$$

then upon integrating

$$x = \frac{1}{k} \ln (1 + kv_o t)$$

solving for v_o

$$v_o = \frac{e^{kx} - 1}{kt}$$

Both v_o and k are to be calculated from this derivation. Three (x , t) points provide sufficient information to make this possible. Given three (x , t) points measured by the spray particle velocity measuring system, the equations appear as follows:

$$v_o = \frac{e^{kx} - 1}{kt}$$

$$v_o = \frac{e^{kx2} - 1}{kt_2}$$

$$v_o = \frac{e^{kx\,3} - 1}{kt_3}$$

By a process of iteration, the decelleration factor k and the initial velocity v_o may be found that satisfy all three equations simultaneously.

The k obtained as outlined above is a drag coefficient which is related to the aerodynamical drag coefficient in the following way:

$$k = \frac{\rho AK}{m}$$

where

ρ = density of the surrounding atmosphere (air remaining in vacuum tank)

A = area presented to the air by the spray particle

m = mass of the spray particle

K = aerodynamic drag coefficient

When no air cap forms, as in this case, K = 1.

It is now possible to put in known values for constants in the above equation. When this is done (density of air and steel, and the value for K) the diameter of the spray particle becomes

$$d = \frac{2.9 \times 10^{-7} \rho \text{ (in mm of Hy)}}{k} \quad \text{cm}$$

4.3 Spray Particle Velocity

Also, once k and v_o are determined, the velocity at any point on the trajectory may be calculated from the relationship.

$$v = v_o e^{-kx}$$

When x is taken as the point of impact, the impact velocity v_i may be calculated.

4.4 Effect of Viscous Forces

When the deformable liquid steel particle strikes a solid, the forces which come into play are rather complicated and are not completely understood. Neither are there any fully understood scaling laws which allow one to describe macro-effects from micro-effects and visa versa. It is however known that inertial forces, equation of state pressures, and material strength forces seem to scale linearly. If these were the only forces involved, the ratio of crater dimension to pellet dimension would be independent of pellet size at a given velocity. On the other hand, viscous forces scale in such a way that their influence increases for smaller apparata.

To illustrate the effect of the viscous force by analogy, consider a sphere moving through a viscous fluid. By Stokes law, the drag force on it is,

$$\text{Drag force} = 6\pi r \eta v$$

where r is the radius of the sphere, η is the fluid viscosity, and v is the sphere velocity. When we divide both sides of the equation by the mass of the sphere, we arrive at the sphere decelleration.

$$\frac{dv}{dt} = \frac{9\eta v}{2\rho r^2} \qquad \rho = \text{density of sphere}$$

Upon integration the range of the sphere is

$$\text{range} = \frac{2v_o \rho r^2}{9\eta}$$

for clarity both sides are divided by the radius of the sphere

$$\frac{\text{range}}{r} = Cr \quad \text{where } C = \frac{2v_o \rho}{9\eta}$$

It is seen, then, that the ratio of the range to the radius of the sphere is directly proportional to radius of the sphere.

The spray particle case of a deformable liquid drop impacting into a solid is much more complicated than the above exercise. Nevertheless, the above illustration will help to see how, in the general way, viscous forces should scale. If a centimeter size pellet is stopped in 10 radii by viscous forces, a micron size particle would be stopped in 10^{-3} radii leaving essentially no crater at all. Put in another way, if viscous forces are significant in a hypervelocity impact involving macro-pellets, they will be overwhelmingly dominant for micro-pellets.

A critical test for the relative effect of viscous forces in an impact may be found in a spray particle impact. The measurable parameter of spray particle craters is the diameter (D). The diameter (d) of the micro particle is also known from the above calculations. The ratio of $\frac{D}{d}$ may now be plotted against impact velocity. When spray particle data are plotted along with macro-particle data, the effect of viscous forces, if any, may be readily seen.

5. MEASUREMENTS

One hundred per cent of the research effort was expended in the study of the effects of cratering by particles whose size was in the micron range and whose impact velocity ranged from 4 to 9 km/sec. This effort was unequally divided into three main areas: the means of measuring the time of flight of spray particles and the related project of increasing the velocity were the phases of the research effort which absorbed most of the research attention. The next area of research was that of correlating the particle whose size had been calculated with the crater it produced. The final area of effort was in studying the secondary crater itself.

5.1 Time of Flight of Spray Particle

The system devised to measure the time of flight of a spray particle can best be discussed using a diagram. The diagram in Figure 13 is the original sketch of a spray particle range but later variations on this plan differ only in detail not in principle.

The spray particles are generated at point (1) on the primary target which is the point of primary impact. A portion of the spray particles (preferably only one particle) are allowed to pass through the entrance slit (4), in front of the light pipes (5), and on to the secondary target (3). The spray particle is luminous as it travels through the atmosphere and therefore can be seen by the photomultipliers which look through the light pipes. The location of the particle in front of the light pipe is pinpointed by a double-slit system. Only light which passes through both the slits, one on either end of the light pipe, is allowed to fall on the photocathode. The output voltage of the photomultiplier is displayed on the trace of an oscilloscope. The velocity is calculated from the known distances from the point of primary impact to the light slits and the time of flight of the spray particle to those slits as measured from the oscilloscope traces. This means of measuring the time of flight of the spray particle as it traverses the range is simple in principle but in these short distances and high velocities certain assumptions taken for granted may not be

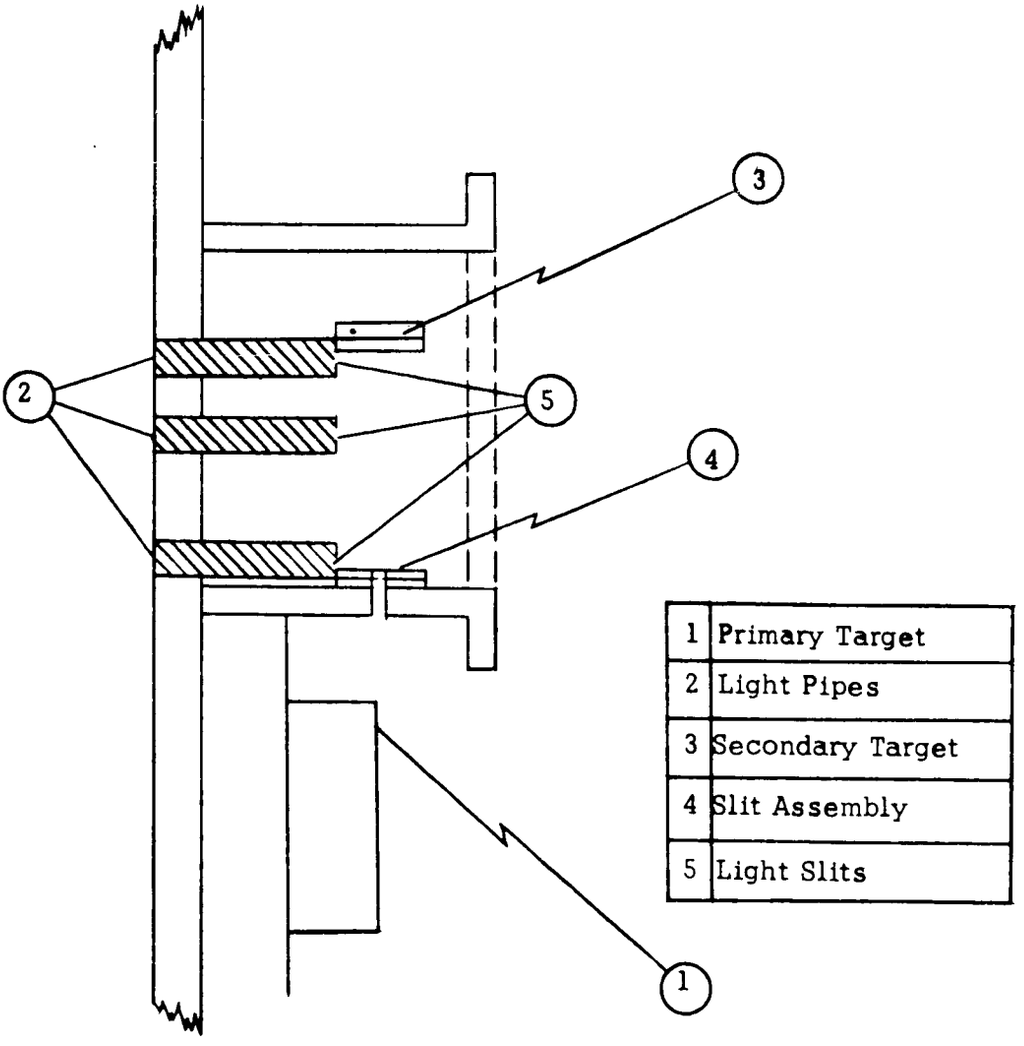

Figure 13 - Spray Particle Target Assembly

valid. It is assumed that the spray particle is launched from the point of primary impact at the instant of the primary flash. This is likely a valid assumption because the light immediately around the pellet at impact (Figure 14) is likely due mostly to spray which is interacting with the atmosphere. The smallest spray particles give up their kinetic energy in collisions with air molecules and either glow or burn brilliantly. The larger particles which maintain their integrity travel into the velocity measuring range. The time involved in the launching of spray from a forming primary crater was not measured but it seems certain that the very high pressures presumably required for launching spray particles can last at most during the time it takes for sound to travel across the pellet; about 0.7 microsecond. If this is true, the worst error in measuring the time of flight would be about 1 %. This is better than it is possible to measure the time from the oscilloscope trace.

A second assumption was that when only one or two craters were discovered on the secondary target and when there was evidence on the oscilloscope trace that one or two flaring particles passed in front of the photomultipliers, the craters were caused by the same spray particles whose velocity had been measured. At the pressure range of 6-10 mm Hg this assumption is likely valid. For example, a spray particle was measured to have an impact velocity of 6.0 km/sec. The diameter of the particle was calculated to be 3.6 microns. The predicted crater size was 23 microns and the measured crater size was 20 microns. This corresponded with theory very well and lent credence to the calculations. On the other hand, when the pressure was reduced to 10^{-4} mm of Hg the impact velocity was still in the 5 km/sec range but the particle diameter was calculated to be approximately 0.04 microns. The calculated crater diameter was roughly five times that, or 0.2 microns, which was too small to be detected with 400X microscope. Nevertheless, craters were discovered on the target which were about the same diameter as the craters seen at the higher pressure.

The explanation given for this seeming quandry was that the spray particles which could be detected were those that would be heated to high enough temperatures by impacts with the air molecules to be molten and for the outer surfaces to be evaporated away. At 6 mm

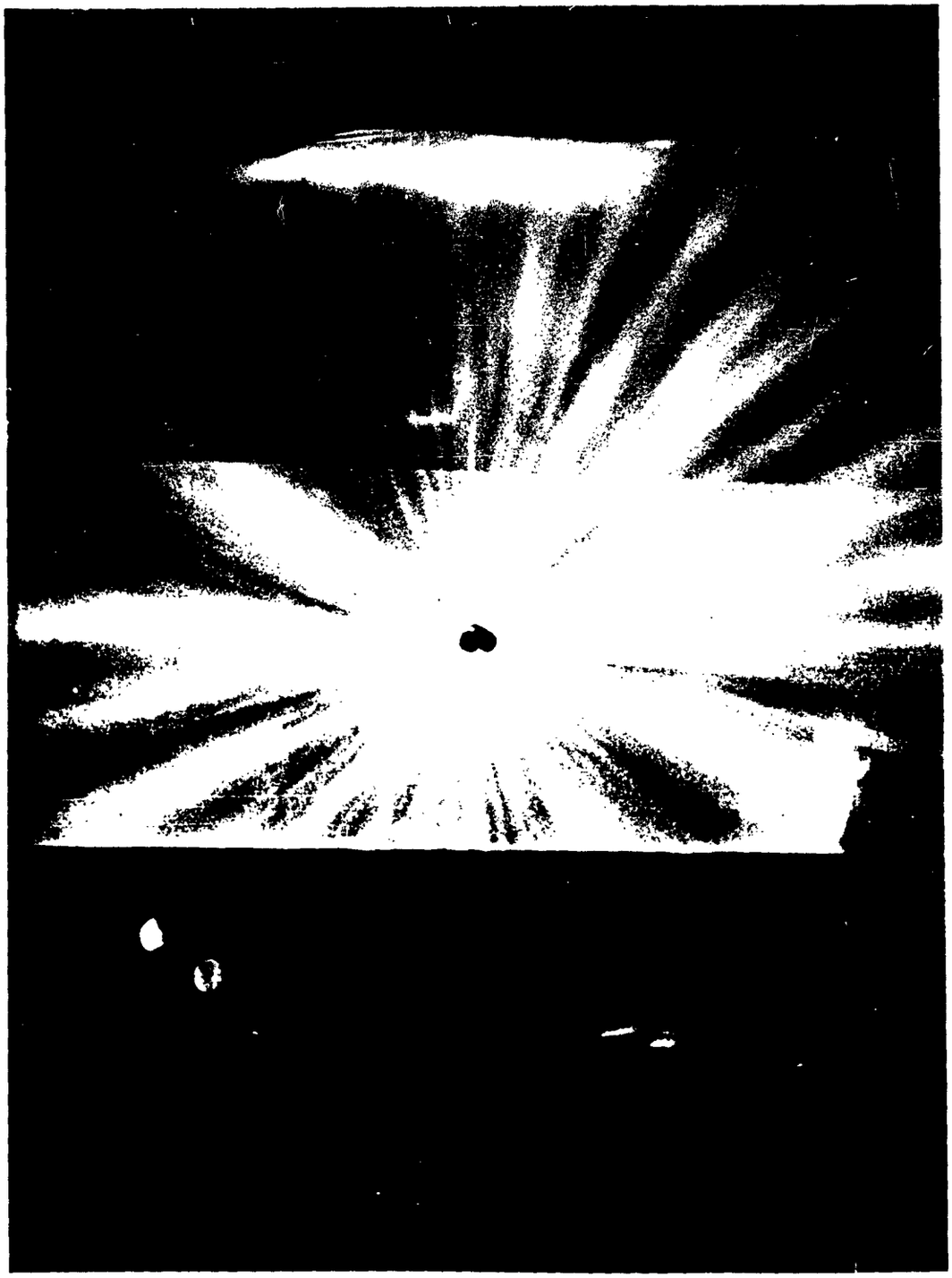

Figure 14 - Hypervelocity Impact Flash

of Hg the smallest particles are stopped and the particles in the 1 to 10 micron range are visible. At the exit angle chosen there are no larger particles generated. When the pressure is reduced to 10^{-4} mm of Hg there are many fewer collisions with air molecules hence much smaller particles become visible. These particles would be stopped at the higher pressure so their presence would never be known at the secondary target. This is not the case with the ever-present larger particles. Even though the larger particles do not become heated enough to become visible, they still pass through the system and impact on the secondary target. The craters seen are made by those and not the particles whose velocity and diameter had been calculated. There were no valid impact data shots made at the 10^{-4} mm of Hg pressure range because of the above described problem.

A third assumption made was that the Öpik drag relationship is valid for calculating velocities in this velocity range. With the limited amount of data obtained during this program, it is impossible to rigorously test the validity of the Öpik theory. On the other hand, there is no reason to doubt it from the results of the experimentation herein reported.

As would be expected, when several spray particles enter the entrance slit of the spray particle range each impacts on the secondary target at its own individual impact velocity. Figure 15 is a graph of data taken from a typical shot. Four particles were discernible from the oscilloscope trace. The distance to the photomultiplier slit is known and the time of flight of the particle can be measured from the trace. When the average velocity for each particle is plotted against the distance traveled, the graph in Figure 15 is produced. As is seen, particle (a) barely slowed down in the length of the range. Particle (d), a much smaller particle, was radically affected by the atmosphere and possibly evaporated before impacting. It is interesting to note that all of the particles seem to have nearly the same launch velocity although their velocity at impact is very different.

5.2 Factors Which Affect Velocity

There are several factors which affect the velocity and character of spray particles. Probably the factor which has the most

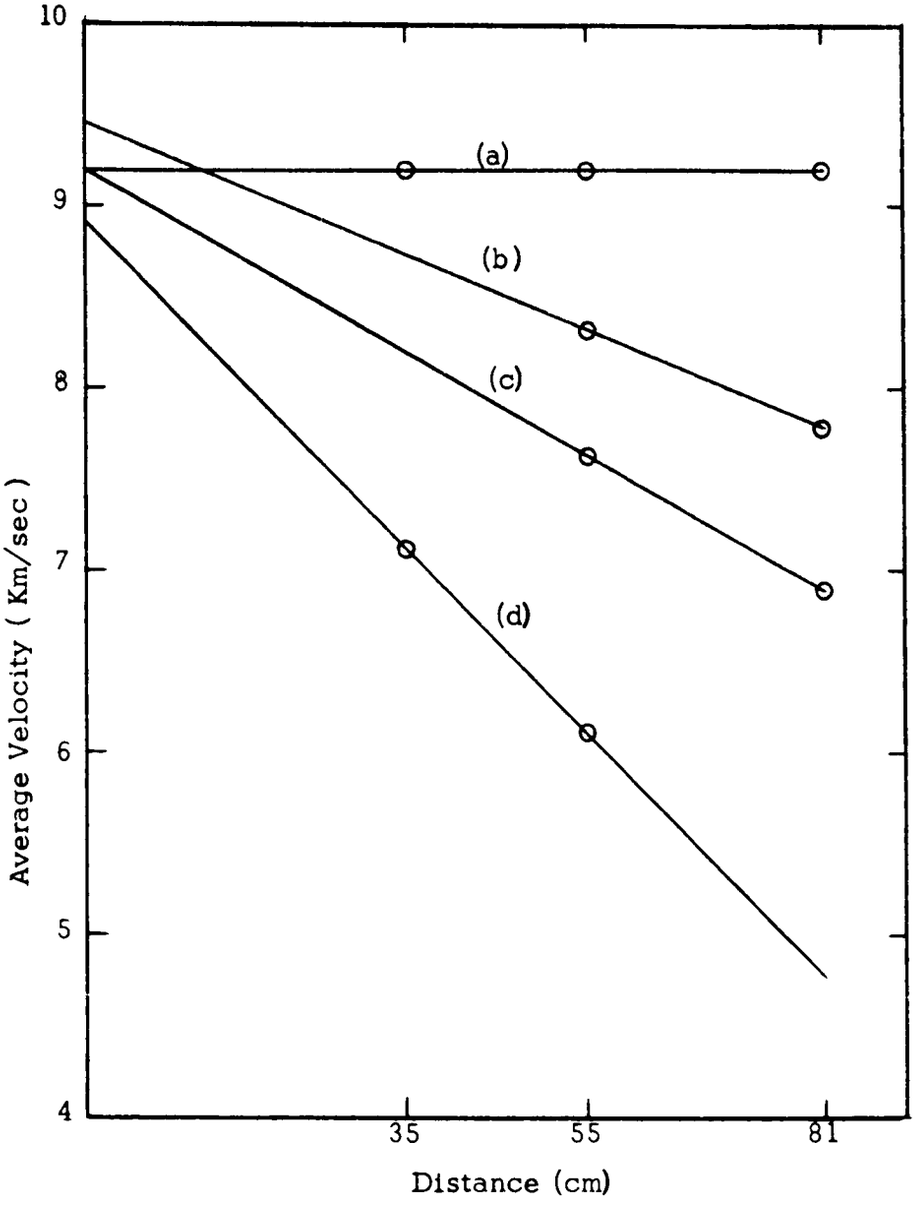

Figure 15

Drag Plot of a Typical Shot

affect on the impact velocity is the tank pressure or the pressure of the air through which the particle must pass to arrive at the target. These investigations have shown that the most important role of tank pressure is that of selecting the particles which will be visible. Those particles which are too small in a given pressure range will be stopped in a very short path length and they will not enter into the experiment. Those which are larger than some maximum size which is determined by the pressure will not be visible because they do not become sufficiently heated. Those in the proper size range become visible and are available on which to make measurements.

A second role of pressure is less well understood. In some yet to be explained way the air present at the point of primary impact has an affect on the size of the spray particles ejected at a given angle. Open-shutter photographs of impacts in the open air show streamers of light more than 20 cm long extending out from the impact point in the region no more than 5° out as measured from the face of the target. Trails as long as these in open air of necessity indicate very large, even macro-size spray particles. When a particle size distribution study was made at 6 mm of Hg pressure, only microscopic craters--indicating microscopic particles--were found in the region up to 5° as measured from the face of the primary target. No study of the distribution of particle size with angle was made at the 10^{-4} mm of Hg pressure.

Another factor which affects the velocity of spray particles should be the amount of energy available in the primary impact. Since the amount of energy in the primary impact varies as the square of the impacting velocity of the primary pellet it was assumed that higher velocities would come when the light-gas gun was used as a launcher for the primary pellet. Whether higher velocity spray results when higher impact energy is available was not fully investigated. The inaccuracy of the light-gas gun made this study extremely difficult. Preliminary shots were, however, encouraging. Measurements not on individual particles but on the advancing front of the fastest particles indicated particles traveling possibly 12 km/sec at distances up to 30 cm from the point of impact.

The two factors of range pressure and pellet velocity can possibly be joined by a third, pellet-target material, which also may

affect the velocity and character of spray particles. When dissimilar materials are used for pellet and target, the spray from the impact is invariably from the less dense material.

The use of materials lighter than steel, such as aluminum or glass, for spray particle work, was suggested as a means of attaining higher launch velocities. Some early work at the University of Utah High Velocity Laboratory [2] indicated that launch velocities on the order of 25 km/sec could be produced from a glass-into-glass primary impact. On the basis of this encouraging work, several attempts were made at Utah Research and Development Company to attain such high launch velocities but the achieved velocities were in the 9-10 km/sec range. Later work at HVL disclosed there had been a wrong oscilloscope setting and that the previously reported 25 km/sec particle velocities were in error. The spray particle velocities there were also in the 10 km/sec range.

5.3 Size Distribution of Spray Particles

In order to calculate the energy of a spray particle as it impacts on the secondary target it is necessary to know both the velocity and the mass of the particle. The material of the spray particle is known because only one material is available. The same material (steel in most cases) is used in both the pellet and the primary target. The mass of the spray particle is the product of the density of the known material and the volume of the spray particle. The mass then is proportional to the cube of the diameter

$$m = \frac{\pi}{6} \rho d^3$$

m = mass of spray particle

ρ = density of steel

d = diameter of spray particle

The diameter (d) or mass of the particle enters into most data plotting schemes presently recognized. When crater volume is plotted versus

pellet energy the mass is involved. The diameter is necessary when plotting the normalized penetration (P/d) versus velocity; and again when the normalized crater diameter (D/d) is plotted versus velocity.

The diameter of the spray particle cannot, of course, be measured directly. The diameter must be calculated from the Öpik drag relations. A discussion of this procedure was found under Theory.

The diameter of a spray particle, and hence its mass, can only be calculated for particles which are visible. The arguments that were mentioned in the discussion of the spray particle velocity above, are valid here as well. The pressure of the tank or the pressure of the range atmosphere determines upon which particles measurements may be made. The tank pressure determines, also, to some extent the mass distribution in angle. When the exit angle of the spray particle is measured out from the face of the primary target, it is seen that large particles (those capable of traveling 20-40 cm in air) are present in the 0° - 10° region at standard pressures. When the pressure of the range is reduced to 6 mm of Hg there are no particles capable of creating visible craters in the first 5° and no particles of the size to travel any measurable distance at atmospheric pressure are found in the first 15°. These observations are only qualitative and were noted in the process of other investigations. No quantitative measurements were made.

Any further discussion of the mass distribution of spray particles in size or in space must be confined to a measure of the craters of their impact on the secondary target. The size of the crater is a measure of the mass or diameter of the particle as long as the velocity is constant. When the spray particle velocities of several particles are measured in the same shot the impact velocities are seen to vary from near 3 km/sec or less, up to the initial velocity which may be as high as 15 to 16 km/sec. It is, therefore, almost impossible to get more than just a qualitative idea of the particle diameter from viewing a multitude of craters for which the impacting velocity is unknown. Nevertheless, larger particles are slowed least by atmospheric drag and the smaller particles are slowed most. Hence, a qualitative picture for particle size may be obtained from viewing the formed craters even if a quantitative picture cannot. In the following

discussion of size and angle distribution of mass the above objection has been considered.

The diameter spread of the spray particles ejected from a primary impact of steel-into-steel in air at 6 mm of Hg pressure and where the impact velocity is 2.2 km/sec is very wide. The craters extend in size from beyond the limit of visibility of the 400X metallographic microscope to well over 300 microns in diameter. The craters throughout the range maintain the characteristics of a crater made by a smooth sphere. The craters are perfectly round. The crater lips are delicately curled out and rise high above the original "ground level." Throughout the size range the craters are easily recognizable because of the foregoing characteristics. The particle diameter that may be assigned to a given crater diameter is a little ambiguous but should be on the order of 0.5 micron for 1.5 micron craters up to about 30-50 microns particle diameter for craters in the 250 micron diameter size. Craters larger than about 250-300 microns in diameter cease to have the characteristic symmetrical appearance. The craters begin to look more like gouges made by some asymmetrical object moving slowly--perhaps 1 km/sec.

5.4 Spatial Distribution of Spray Particles

In the foregoing example the distribution in space is also interesting. In the very small angles, less than 5° as measured out from the face of the primary target, there are no craters discernible to the naked eye. All the craters are microscopic, and they are relatively few in number. As the ejection angle increases so does the maximum size of the crater until some angle is reached which marks the end of spray damage. The number of craters per unit area of secondary target also increases with angle until an angle of about 20° is reached, when the population begins to fall off with angle. There is no loss of small craters as the larger craters come into play. The angle which claims the maximum crater population also has the greater number of craters less than 5 microns in diameter.

The craters are not evenly distributed in space per given shot. They are grouped in "rays" or fingers. Figure 14 is an

open-shutter photograph which shows very well these luminous rays which extend out from the crater. Figure 16 is a sketch of the side view of one of these streamers to show how the spray particles are spread out in angle from the face of the target. It should be pointed out that the area between the rays or fingers are not denuded of craters, there are just fewer craters per unit area of secondary target there.

5.5 Crater Diameter

A knowledge of the crater parameters is fundamental to this investigation. Some of the parameters are easily obtainable while others were difficult to measure. With the equipment available, it was possible to directly measure the diameter of the crater and the outer diameter of the crater lips. It was much more difficult to measure the particle penetration into the secondary target or to measure directly the volume of the spray particle crater.

The diameter of the crater formed at impact of the spray particle on the secondary target was measured directly on the metallographic microscope. The calibrated scale in the eyepiece of the instrument made possible precise measurements at any desired magnification up to the limit of magnification of the microscope. Most measurements were made visually but when deemed necessary a photographic record was made, also with the scale visible.

Early measurements were made by photographing the crater while focusing the microscope on the lips of the crater. It was soon seen that the focus should be made at "ground level"--the original level of the secondary target surface before impact--and the diameter of the crater measured should be the diameter of the in-focus circle. It was felt that this improved method of measuring gave a more accurate picture of the crater diameter and made a difference of about 30% in the measured diameter.

The spray particle crater is accurately circular at "ground level." The lips of the crater rise above "ground level" then as the microscope is focused deeper into the crater the sides gently slope inward until a round bottom is reached. Although the depths of

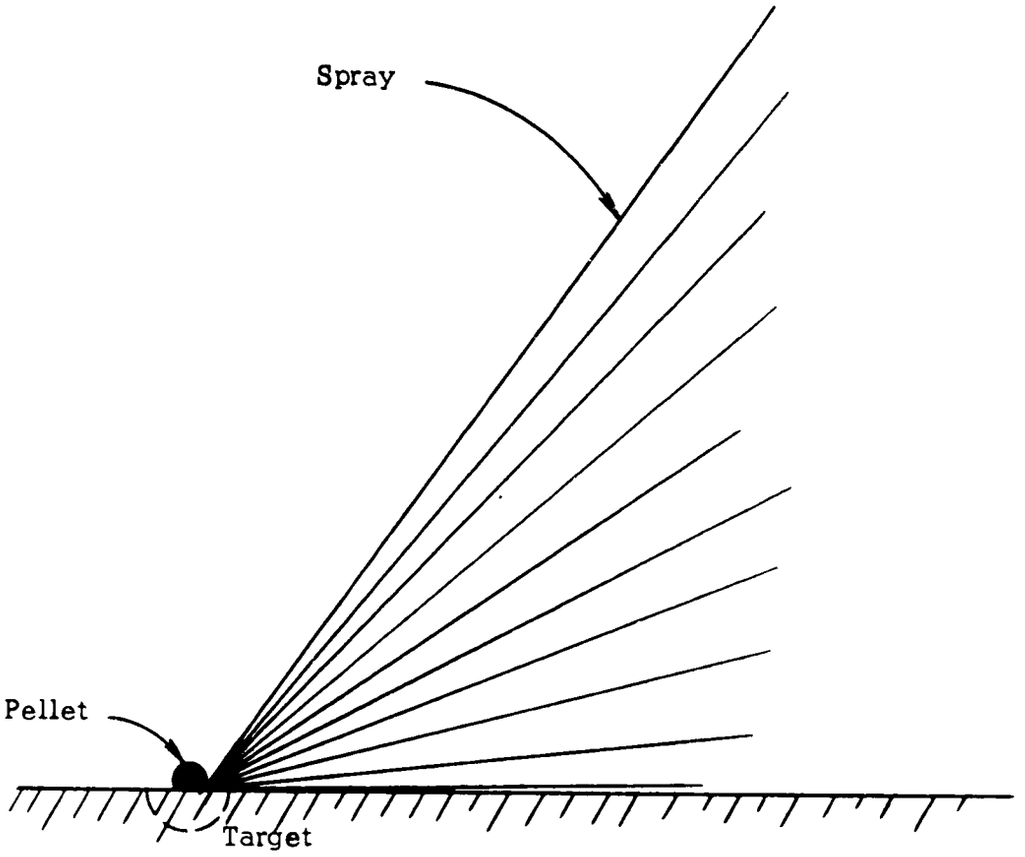

Figure 16

Profile of a "Ray" From a Primary Impact

the craters cannot be measured with present equipment, most indications are that the craters are hemispherical in shape, at least for the higher velocity impacts.

5.6 Penetration and Volume

Two schemes were tried to measure the penetration and the volume of the micro-craters. An attempt was made to section the craters by metallographic techniques thus being able to measure their depth directly. Figure 17 and Figure 18 are examples of this approach. These pictures were made from a target which had thousands of micro-craters on it. The technique was to cut off a portion of the target and mount it in plastic so that the side being polished was at right angles to the original face of the target. It was found that in the polishing process the plastic mount was worn away more quickly than the metal. When the polished side was placed on the microscope, it was seen that the edge of the metal on the boundary between the plastic was neatly rounded completely obliterating any craters that might have been there.

The next attempt to section the micro-craters used a similar technique except that the face of the target that contained the craters was placed against a flat piece of the same type aluminum. The polishing then cut both pieces of aluminum equally and it was possible by a process of polishing and examination to eventually discover a crater that looked like it had been sectioned.

There was no way to control the cutting depth of the polishing. The 600 grit that gave a very good shine to the aluminum was unsatisfactory because the grit was of the same order as, or larger than, the craters in question. When a slice was taken off by the polish, it became pure luck if there were a portion of a crater cut away revealing the crater profile. When the finer diamond paste was used, the same problem remained. It was impossible with URDC equipment to control the cutting depth on the polishing process to accurately slice away one half of any micro-crater even when there were thousands available, let alone polish down to one single crater for which the particle size and impact velocity were known, and section it at dead center. Another approach had to be sought.

Figure 17

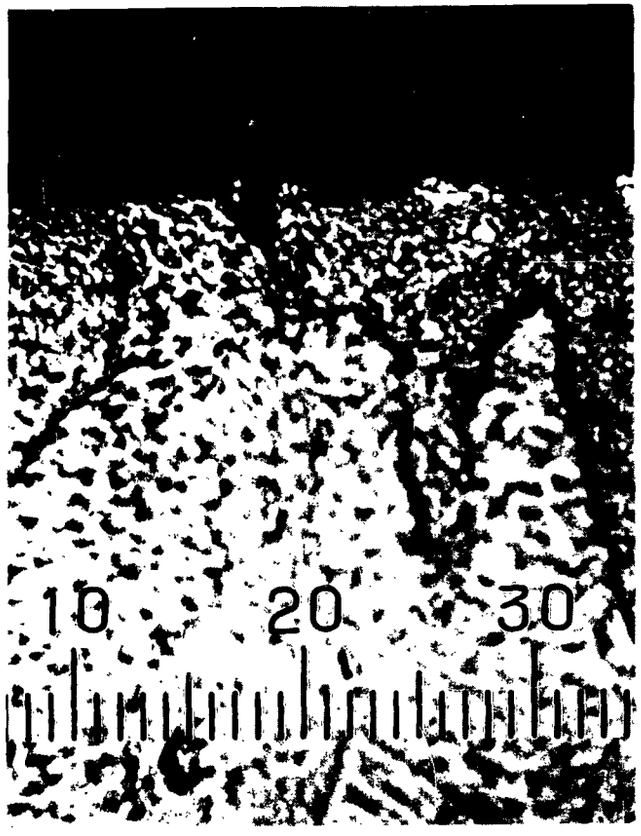

Figure 18

Sectioned Spray Particle Craters

Two other methods were suggested, neither of which were seriously attempted because the equipment was lacking. The first was to calibrate the focus. The depth of field at magnification in the metallographic microscope was very shallow. It was suspected at first that a scale could be mounted on the fine focus knob and calibrate this for depth. It was all too soon discovered that there was too much backlash in the gearing of the focusing mechanism to be able to calibrate it successfully.

The second method suggested to measure the penetration, volume, and shape of the crater was to use an electron microscope. Nothing was done in this regard because there is no electron microscope immediately available to URDC.

5.7 Size and Angular Distribution of Craters

A study was made of the size distribution of the craters made by the spray from a primary impact. Figure 19 shows diagrammatically the experimental setup. The secondary target was placed on the chord of a three-inch circle whose center was the point of primary impact. The targets were four inches long and one and one-half inches wide. Figure 20 is a picture of the face of one of these targets after the shot. The lower end of the target in the picture contains craters so microscopic that they are not visible at this magnification.

There are several important points to note from this picture which are typical of all of the shots made. The first point noted is the limit of the visible craters. It was discovered that in the first five degrees or so measured up from the face of the primary target, there are no visible craters. A cursory look with a magnifying glass disclosed a wealth of craters, however, which were too small to be seen with the naked eye. These extended as nearly as could be determined to the line that marked the plane of the face of the primary target. They were not evenly distributed. The same apparent grouping into fingers or rays of craters that are seen in the visible craters extend down into the microscopic craters.

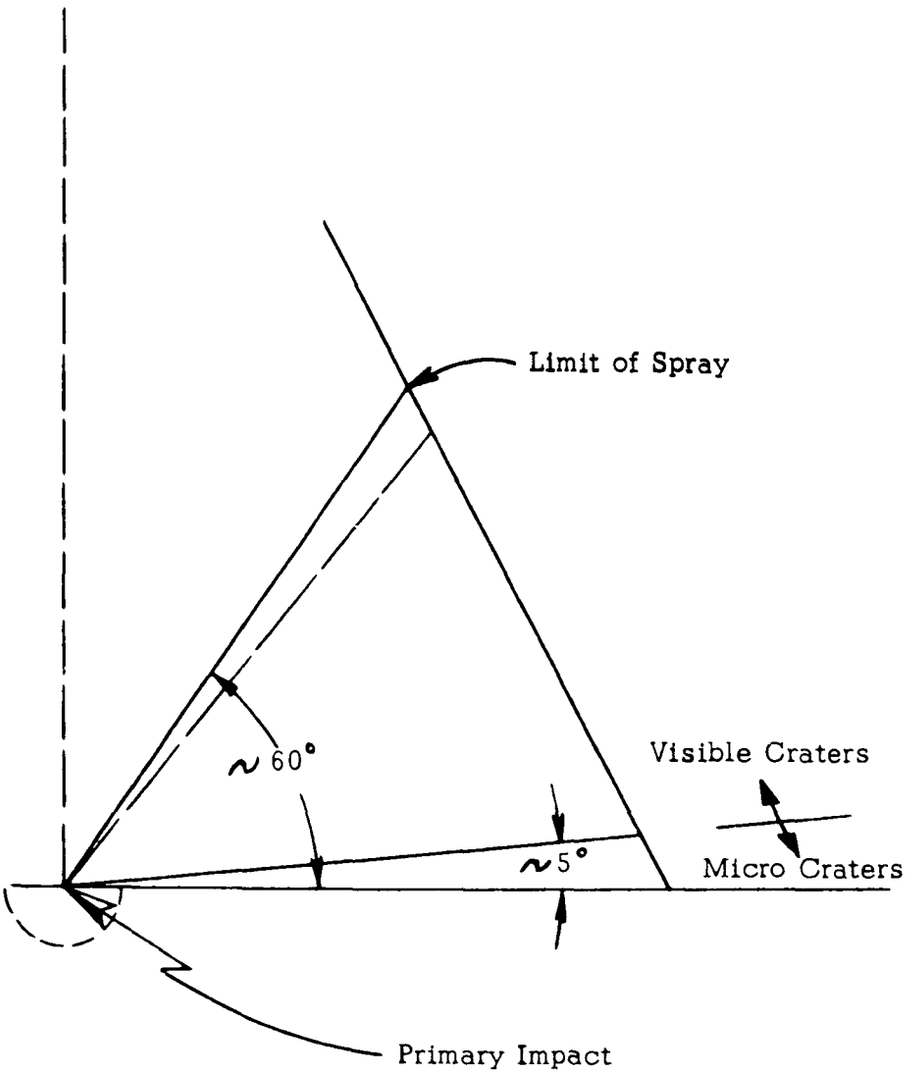

Figure 19
Target Location for Spray
Distribution Investigation

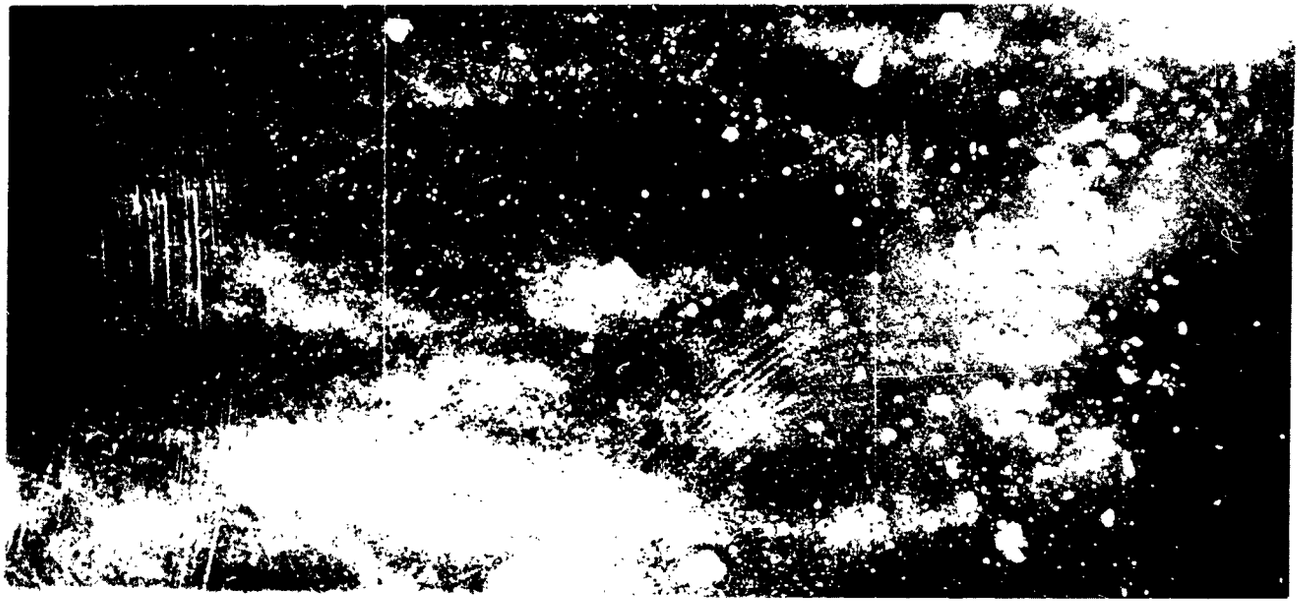

Figure 20 - Spray Particle Craters

The second point to note is the existence of the rays or grouping of craters in long chains instead of being evenly distributed over the target. This grouping is more obvious on the actual target than can be seen on the picture.

A third point of interest is that although the visible craters begin at about five degrees the microscopic craters continue to be present also. It was anticipated that the micro-particles which cause the micro-craters would be present at right angles to the flight path of the primary projectile. It was also anticipated that the larger particles would become available as the angle up from the face of the primary target increased. It was not anticipated that the micro-particles would also be available in the region from five to twenty degrees. By coincidence the greatest concentration of spray particle craters both visible and microscopic came at about 20°.

The greatest concentration of craters does not mean the greatest damage to the target. The largest spray particles which now become spall concentrate in the angles from 45° to 55° as measured from the face of the primary target. There are some scars on the secondary target from spall elsewhere on the secondary target as is seen in Figure 20, but the greater portion of spall damage is in the 10° region from 45° to 55°. The craters made by the spall do not have the same characteristic shape of the regular spray particle craters. Rather the craters made by the spall appear as gouges as if made by large irregular-shaped pieces.

The limit of spray damage from steel-into-steel impact whose impact velocity is 2.2 km/sec is seen to be at about 60° as measured out from the face of the primary target. The number of craters drops down markedly at that point and the targets appear to be undamaged beyond 60° or so.

An effort was made to make a more quantitative investigation of the distribution of the micro-craters. The small one-inch diameter disc that had been used for a secondary target was replaced by a block of aluminum six inches long and whose target area was one inch wide. The target block can be seen mounted on the stage of the metallographic microscope in Figure 21. The large target

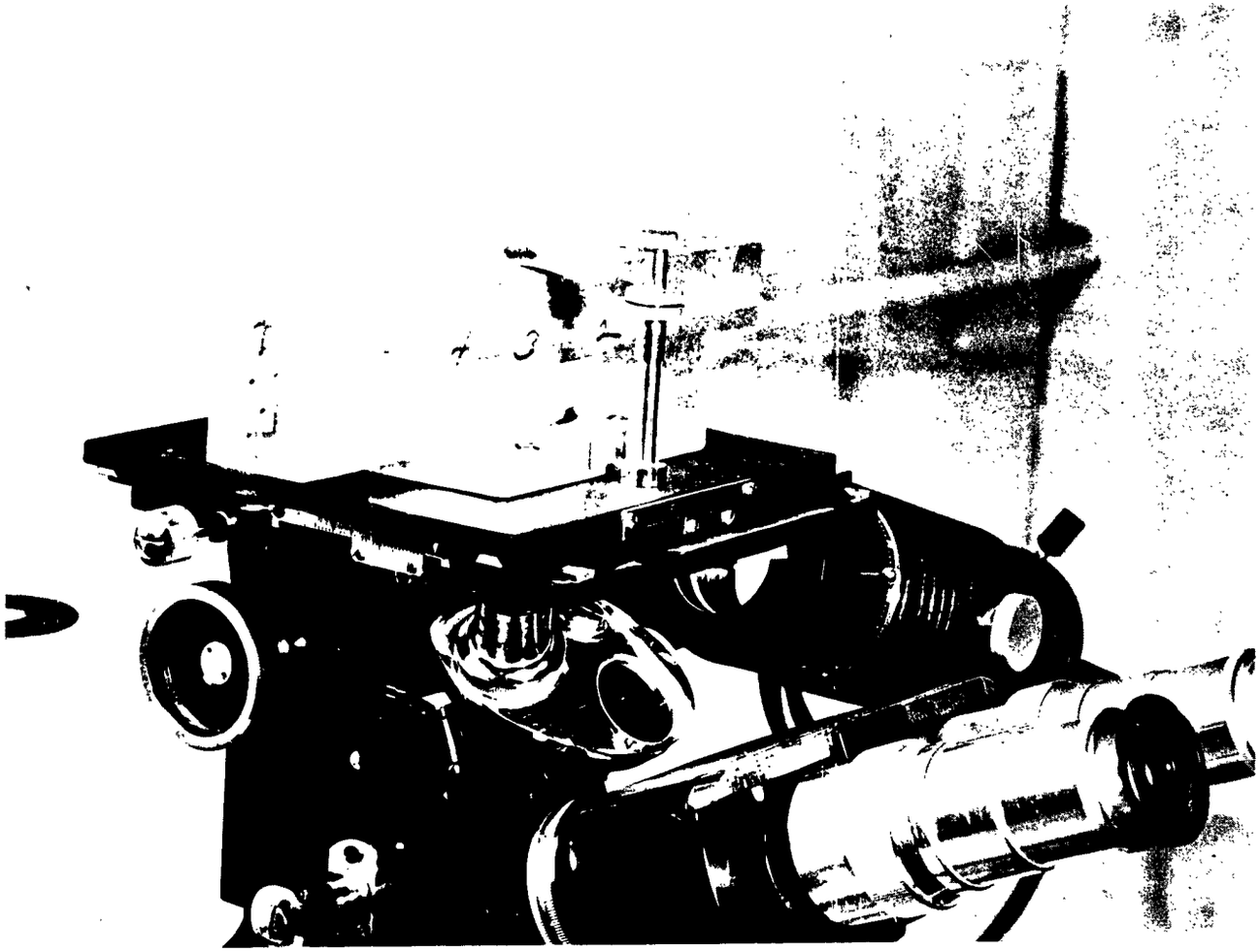

Figure 21 - Specimen (Target) on Microscope

intercepted about 50° as measured out from the plane of the face of the primary target. The face of the target in the long direction was parallel to the line of fire of the primary projectile. Figure 22 shows in diagram the test setup. Instead of using the tiny aperture normally used in the old range the full two and one-half inch length of the slot was used. Thus none of the area of the large secondary target was masked.

The ray or finger-like effect of crater distribution from single impacts led the investigators to distrust the sampling from a portion of the spray from a single impact as being representative. In order to get representative distribution of spray particle craters on the target, four shots were fired and spray from all four shots impacted on the same area of the large target. The sampling technique was to count all of the craters in a strip 250 microns wide, across the full width of the target. The total number was then divided by four to get an average number per shot. Sample strips were chosen at regular intervals along the large secondary target and the craters were counted in each strip.

In order to see the distribution (Figure 23) in size as well as in number, the craters were counted in three groups. All craters from 5 microns down to the limit of visibility at 100X magnification were counted in one group. The second group contained all of the craters between 5 and 25 microns. The third group was made up of craters larger than 25 microns in diameter.

This sampling method was adequate to get a representative picture of the small craters but undoubtedly was unsatisfactory to show a representative distribution of the very large craters and the "gouges" made by spall. The craters of interest in this study were the small craters because they represented impacts by spray particles. The distribution of spray particles as a function of both size and angle from the plane of the face of the primary target were seen very clearly. It is possible that a more clear picture of larger crater distribution in size and angle could have been obtained by reducing the magnification on the microscope and by using a wider sampling strip. This was not done because the larger particles were not of particular interest at the time in this study.

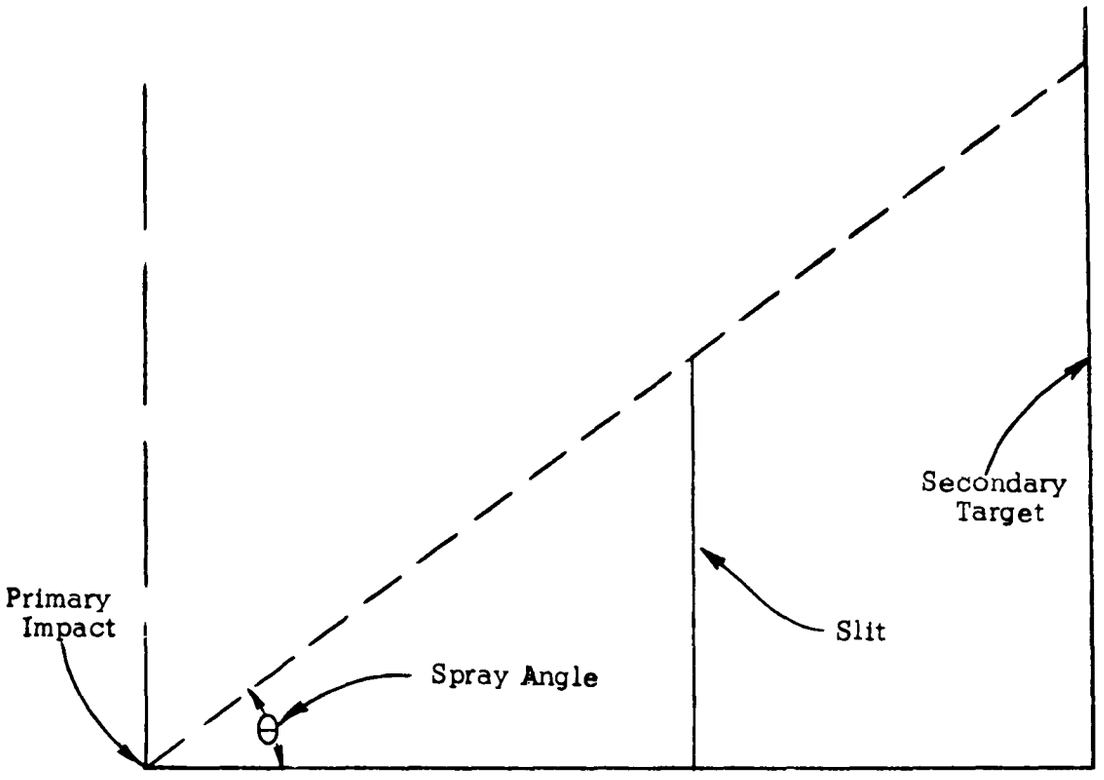

Figure 22
Diagram showing relative position of
impact slit and secondary target

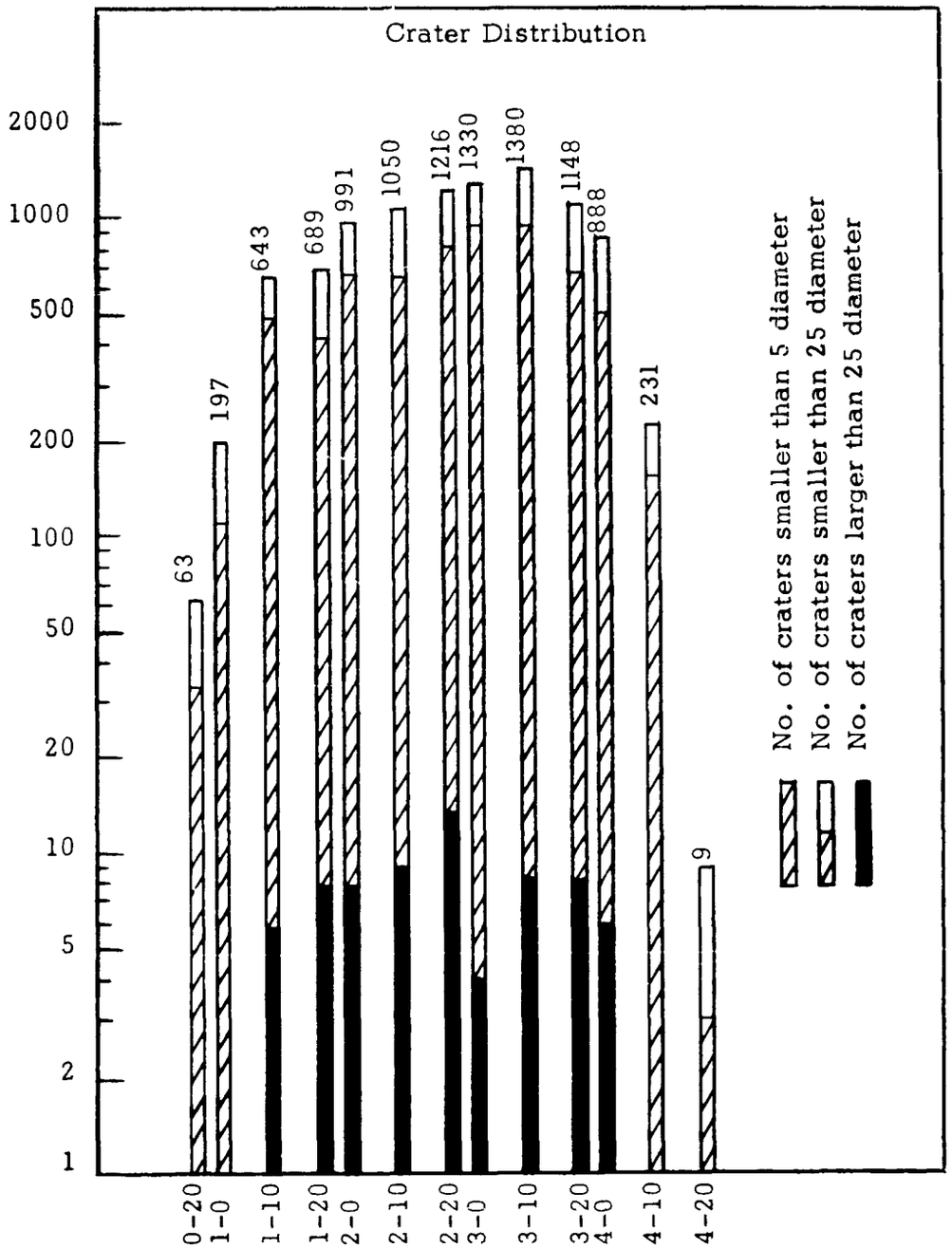
Crater Distribution
2000
1000
500
200
100
50
20
10
5
2
1
63
197
643
689
991
1050
1216
1330
1380
1148
888
231
9
0-20
1-0
1-10
1-20
2-0
2-10
2-20
3-0
3-10
3-20
4-0
4-10
4-20
No. of craters smaller than 5 diameter
No. of craters smaller than 25 diameter
No. of craters larger than 25 diameter

Figure 23

The sample strips 250 microns wide in which all the craters were counted and totaled in three categories were not equidistant apart. The choice of linear measurement was dictated to a great extent by the stage and the verniers on the microscope. The first strip was 20 mm from the end of the target and 10 mm from the line where the place of the face of the secondary target cut the plane of the secondary target. The third was one inch plus 10 mm; the fourth, one inch plus 20 mm; the fifth, two inches; and so forth to the end of the target. The first sampling strip at 10 mm from the beginning of the craters represents an exit angle of between 2° and 3°. The region of greatest concentration of spray particle craters is approximately 7 cm from the beginning of craters or at about 20° exit angle from the point of primary impact.

It was of interest to know whether the spray particles launched at or near 0° would have velocities higher than those launched at greater exit angles. For purposes of this program, it was important to use the highest velocity particles possible to obtain. The large target was retained and the long slot was masked off allowing only a very small aperture whose position along the slot could be changed. Several shots were fired at several positions along the slot before this phase of investigation was abandoned in the press of time and other seemingly more rewarding work.

6. DISCUSSION OF RESULTS

Dr. Robert Bjork of Rand Corporation [3] has predicted that craters from impacts whose impact velocity is above about 5 km/sec should be hemispherical in shape. If it is true that a hemispherical crater results from an impact whose impact energy is sufficiently high to overcome any forces from the strength of the material, it is then possible to calculate the penetration from the diameter. The penetration is then one-half the diameter and the ratio of the diameter of the crater to the diameter of the pellet is proportional to the usual normalized penetration (P/d) and the volume of the crater is $\frac{\pi}{12} D^3$. The diameter of the crater is presently accurately measurable whereas the other related parameters of the crater are not.

In addition to the above argument for using the ratio of the crater diameter to pellet diameter another argument is also valid. It has been noted that the diameter of the crater mouth increases with velocity regardless of the interior shape of the crater. The crater diameter normalized by the pellet diameter (D/d) was plotted against velocity in Figure 24. The points represented by circles were data taken by Johnson and others at the University of Utah High Velocity Laboratory. In that case, they were shooting 3/16" diameter steel spheres into aluminum targets. The points represented by triangles were taken from data reported by Kineke and his associates at the Fourth Hypervelocity Symposium. The Kineke group fired flat discs off the face of explosives. The impact orientation of the disc was unknown so for this plot it was assumed that the craters were made by steel spheres whose diameter the sphere would have if the sphere had the same mass as the disc. It should be pointed out that if the disc presented an impact diameter to the target that was less than that of the equivalent sphere, the triangle points would move upward on the graph. The data taken from the above two sources was data in which the particles and their craters were in the macro range.

The points plotted on the graph with squares represent the data gathered in this investigation. The particles and the craters were in the micron diameter range. When the ratio of crater diameter to particle diameter is plotted against velocity these points are consistant with and extend beyond the other plotted data.

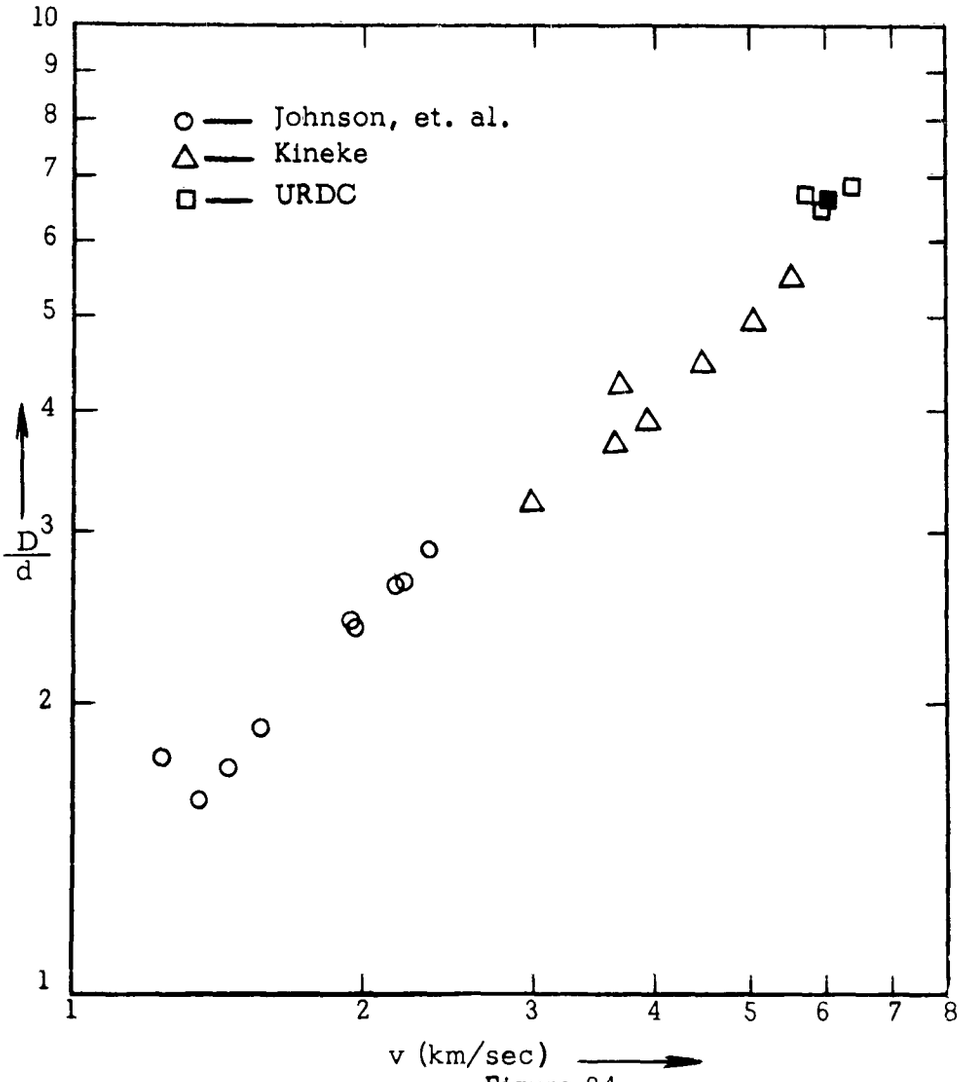

Figure 24
Ratio of Crater Diameter to Pellet Diameter vs. Velocity for Steel into Aluminum

The consistency of the spray particle data with the macro-particle data is especially significant for two reasons: The first significant point is that a scaling law is demonstrated from micro-effects to macro-effects. It is seen the diameter of the resulting crater may be predicted from the impact velocity and the particle diameter regardless of the particle size range involved. This scaling relationship is probably the most important result of this investigation.

A second significant point is that here is strong evidence for neglecting viscous forces, thus simplifying calculations in any mathematical model of hypervelocity impact that might be proposed.

Our evidence indicates strongly that forces proportional to strain rate are not important in crater formation in metals. This agrees with an empirical study made by Hayes International Corporation for APGG, Eglin Air Force Base [4] which shows that the pellet diameter had little effect on the ratio of pellet size to crater size. Their data were much more accurate than ours, but covered a much smaller range of projectile sizes.

Some impact theorists, e.g., T. D. Riney [5] assume a viscous force during cratering and then assume that the viscosity coefficient decreases rapidly with increasing strain rate. Thus they arrive at a shear force, resisting deformation which is approximately independent of strain rate. Our data has no bearing on the question whether such a "viscous" force is important.

7. CONCLUSIONS

Three definite conclusions may be made from the work under this contract. They are as follows:

1. The diameter of a crater made by a particle impacting at a given velocity may be predicted through the normalizing relationship. The ratio of the crater diameter to the pellet diameter is proportional to the velocity (Figure 24). This scaling law is the most important discovery derived from this investigation.

2. This study has shown that forces proportional to the strain rate which should become overwhelmingly dominant in a micro-particle impact, if they are significant in macro pellet impact, are insignificant in both cases and may be neglected.

3. This study has also shown that at the present state of the art spray particles are not satisfactory tools for impact studies. Special techniques must be developed to study in more detail the crater and its surroundings. Some microscope which is calibrated to measure depth must be used to measure penetration directly. Using such a tool the crater shape could be plotted to give a good picture of the volume. New techniques are required also to measure the velocity of spray particles which do not interact with the atmosphere hence do not either become luminous nor slow down. It must be noted here also that single impacts from single particles upon which drag measurements have been made are nearly impossible to obtain.

8. RECOMMENDATIONS

Spray particles appear to be excellent tools for the study of artificial meteorite trails. The trails are brilliantly luminous. They seem to be excited by the same mechanisms that make the trail of a natural meteorite luminous. They are plentiful and easily produced. The particle size range may be chosen arbitrarily by simply selecting the tank pressure which makes the desired size luminous. And finally they can be produced where equipment for their observation is easily placed.

This investigation of spray particle impact has suggested several interesting unexplored fields for further inquiry some dealing with micro-particle impact and some related to the primary impact. It would be very interesting to know the true shape of the micro crater. The elementary metalographic work that was done in an attempt to section some of these tiny craters seemed to show them slightly modified in shape by their position in the grain structure of the metal. Some of the unanswered questions are: "What is the exact shape of the crater (volume, diameter penetration, lip formation, related damage) when the particle impacts at normal incidence to a grain boundary?" "How do these parameters vary when the angle of incidence changes?" "What happens when a particle strikes in a boundry between two grains." "Does the damaged volume decrease or increase with grain size at the surface of the target?" All of these questions need answers to predict micro meteorite damage in space.

Two other fields of investigation suggest themselves from this work that involve the primary impact. The highest possible velocity attainable in the spray from a primary impact is not definitely known. Spray particles with velocities from 4 to 8 times the velocity of the primary impact velocity of 2.2 km/sec have been seen. There is indication that spray from the higher impact velocities of the light-gas gun has a potentially higher velocity but as yet no investigation has been completed which describes how the velocity of the spray varies with primary impact velocity.

An effect that was noted in passing was the presence of spray grouping or rays. The reason for this is unknown and the

significance of them if any is equally unknown. The fact that rays extend from several lunar craters makes rays from impacts increasingly interesting.

These results achieved from spray particle study are a good first step in the use of and the understanding of this tool. More refined techniques and some more specialized equipment would be needed to use spray particles to gain more useful impact information than already found. These studies have pointed out the value of spray particles in trail ionization studies. They also have opened interesting fields for future investigation.

9. REDIRECTION OF EFFORT

9.1 Statement of Problem

The purpose of the redirection of effort for Contract No. AF 08(635)-2099 was two fold. The first aim was to investigate ways and means to obtain data on the total momentum of the backspall resulting from very high velocity penetration and to collect as much of this data as possible. The second aim was to obtain new data on the temperature of the impact flash associated with the impact of the projectile on the target.

The velocity range of the projectiles would be from 15,000 fps to as high as possible. The projectiles were to be 2024T4 aluminum spheres. The targets were to be 2024T4 aluminum plate of various thicknesses.

As can be seen, this is a rather ambitious program wherein the greater portion of effort was expended toward attaining the first aim.

9.2 Method of Momentum Difference

The method chosen to measure the momentum of the backspall was the use of the ballistic pendulum. When the ballistic pendulum is used (See Figure 25) and by the law of conservation of momentum, the following relation is valid:

$$M_S = MV - mv \qquad (1)$$

where:

M_S = Momentum of backspall

M = Resulting mass of pendulum after impact & penetration of the target face by the pellet.

V = Resulting velocity of the pendulum

m = Mass of the impacting pellet

v = Velocity of the impacting pellet

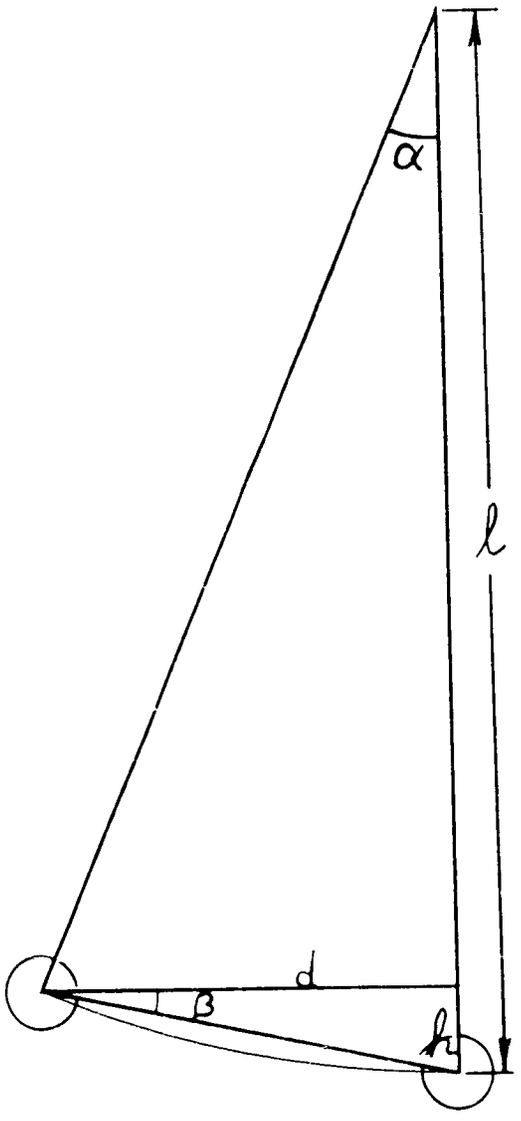

Figure 25

Pendulum

The Kinetic energy received by the pendulum is equal to the potential energy of the pendulum at the top of its swing.

$$1/2\ MV^2 = Mgh \qquad (2)$$

$$V = (2\ gh)\ 1/2 \qquad (3)$$

From Figure 25

$$h = d \sin \alpha \qquad (4)$$

and when α is sufficiently small,

$$\sin\alpha = \sin\beta = \alpha \qquad (5)$$

then

$$h = \frac{d^2}{l} \qquad (6)$$

The period of the pendulum may be described as a function of the acceleration of gravity and the length of the pendulum arm.

$$T = 2\pi\sqrt{\frac{l}{g}} \qquad (7)$$

Solving

$$l = \frac{T^2 g}{4\pi^2} \qquad (8)$$

Substituting into (6) and clearing

$$h = \frac{4\pi^2 d^2}{T^2 g} \qquad (9)$$

Substituting (9) into (3)

$$V = \frac{2\sqrt{2}\,\pi d}{T} \qquad (10)$$

Substituting (10) into (1)

$$M_s = \frac{M\ 2\sqrt{2\pi}\,d}{T} - mv \qquad (11)$$

The quantities to be experimentary measured in (11) are:

d = Linear displacement of the pendulum in the disection of the first swing

T = The period of the pendulum

M = The mass of the pendulum

m = The mass of the projectile

v = The velocity of the projectile at impact

9.3 Direct Measurement of Spall Momentum

Another experiment postulated to measure the momentum in the backspall also made use of the ballistic pendulum. Figure 26a is just one of several possible experimental setups of this type. The pellet would be fired through the hole in the hemispherical bob of the backspall pendulum. The spray and the spall from the impact would be captured on the inside of the hemisphere and the component of the momentum in the direction opposite to the direction of the original pellet may be measured. The argument is similar to that in the preceding section. The momentum of the spall (M_s) is equal to the momentum imparted to the pendulum (MV). As was done before, the velocity of the pendulum can be obtained by measuring the displacement.

Another direct momentum experimental setup would be as seen in Figure 26b. A portion of the spall would be taken through an apperture and the momentum measured. This momentum would then be integrated around the circle to obtain the total momentum of the spall ejected at angle θ.

These and other schemes to measure the momentum of the spall were considered but were not tried because of the lack of time to set up the experiment.

9.4 Black Body Temperature of the Impact Flash

The method chosen to measure the temperature of the impact flash was to make use of what was essentially a two color spectroscope. Two photocells were chosen, one sensitive in the blue region of the spectrum with peak sensitivity at 4000A, the other sensitive in the red with its peak at 8000A. The Planck radiation law says:

$$\Psi_\lambda = \frac{8\pi ch}{\lambda^5} \qquad \frac{1}{e^{\frac{ch}{\lambda KT}} - 1} \qquad (1)$$

Where

Ψ_λ = Energy per unit band width radiated by the black body

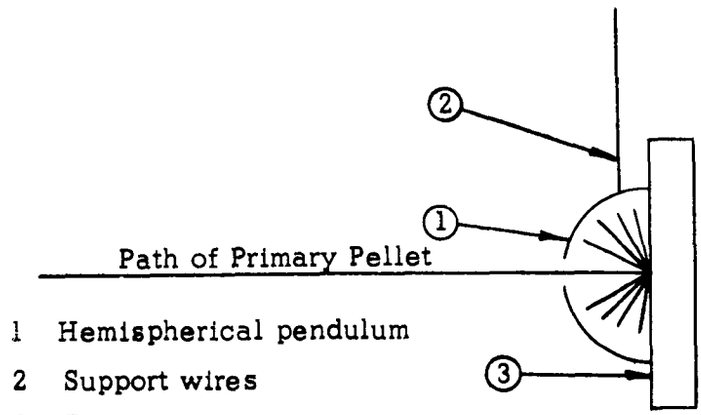

1 Hemispherical pendulum
2 Support wires
3 Target

a.

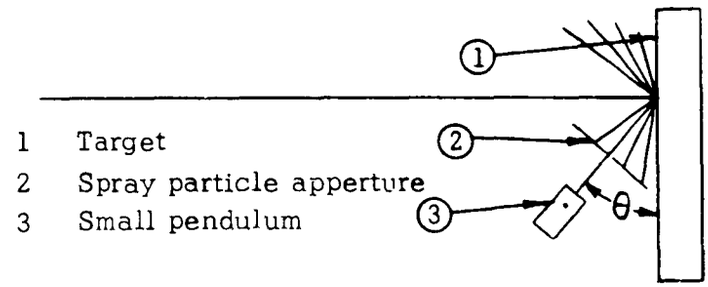

1 Target
2 Spray particle apperture
3 Small pendulum

b.

Figure 26

Direct Measurement of Spall Momentum

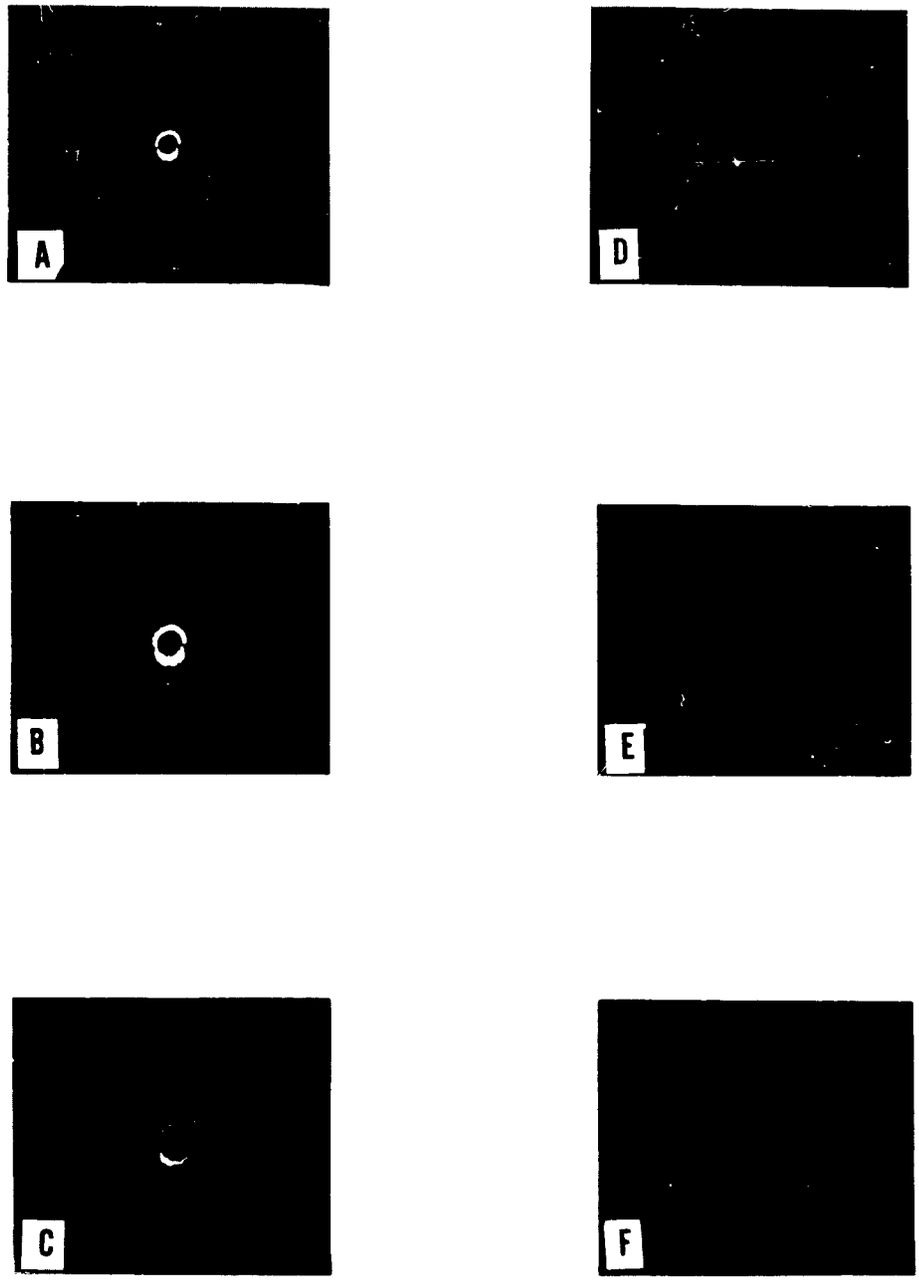

Figure 27 - Kerr Cell Camera Photographs of an Impact Flash

λ = Wave length
c = Speed of light
h = Planck's constant
K = Boltzman's constant
T = Absolute temperature

Since the phototubes have their peak response at the convenient round numbers of 8000A and 4000A or λ and $\lambda/2$, the ratio of the energy received by them from the black body as a function of temperature is

$$\frac{\Psi\lambda/2}{\Psi_\lambda} = \frac{3^2}{e^{\frac{ch}{\lambda KT}} - 1} \qquad (2)$$

When (2) is solved for temperature and the known values for the constants are entered

$$T = \frac{18,000}{\ln\left(C\,\frac{P_R}{P_B} + 1\right)} \qquad (3)$$

where P_R and P_B are the observed outputs of the red-sensitive and the blue sensitive phototubes, respectively. The constant C is determined by observing a source of known temperature.

The above discussion is valid for a pure black body source and is a fair approximation for spectra produced in an impact flash providing the spectrum is not dominated by a single color, ie. the sodium D lines.

There is reason to believe that the great majority of the light associated with an impact flash comes from the interaction of the micro-spray particles with the ambient atmosphere. Figure 27 is a series of photographs showing the expanding " do-nut" of light around the point of impact. It is possible that there is low intensity light in the forming crater that is below the exposure threshold of the film but it is quite evident that most of the light is moving with the expanding cloud of spray particles and not in the crater itself. It is possible, using an optical arrangement with a lens train and stops, to focus only on the crater and screen out all light from the spray particles. This lens system has not yet been constructed. When the lens system is developed, the temperature of the crater light may be measured.

9.5 Experimental Apparatus & Data

9.5.1 Gun and Range

The light-gas gun and the range used in this experiment were described in Part A of this report.

9.5.2 Pendulum

The ballistic pendulum was constructed as seen in Figure 28. The body of the pendulum is 40" long and 5" in diameter. The target may be any size up to one foot square and is mounted on the front. The body of the pendulum is filled with sand to give the pendulum added mass and to act as a catcher for the pellet which penetrates the target.

The pendulum was supported in the classical 5 support wires method. The light shown mounted on the side of the pendulum in Figure 28 is the light by which the displacement of the pendulum was measured. An open shutter photograph of the light from the side gives the double amplitude of the swing. One half the distance between the points of the arc of light is the displacement.

9.5.3 Targets and Pellets

The targets chosen for this investigation were of 2024T4 aluminum sheet and plate. The thickness was to be varied from 0.100 inch to 1.000 inch. The projectiles chosen were also of 2024T4 aluminum and were to vary from 1 to 10 grains. The pellet/target systems were to be matched such that penetration of the target by the pellet would be achieved on 90% or more of the shots. It was assumed that since there was such a latitude of pellet size and target thickness that it was intended that the projectile barely penetrate and that it should be forced to expend almost all of its kinetic energy in the target thus providing maximum energy per shot for the ejection of spall.

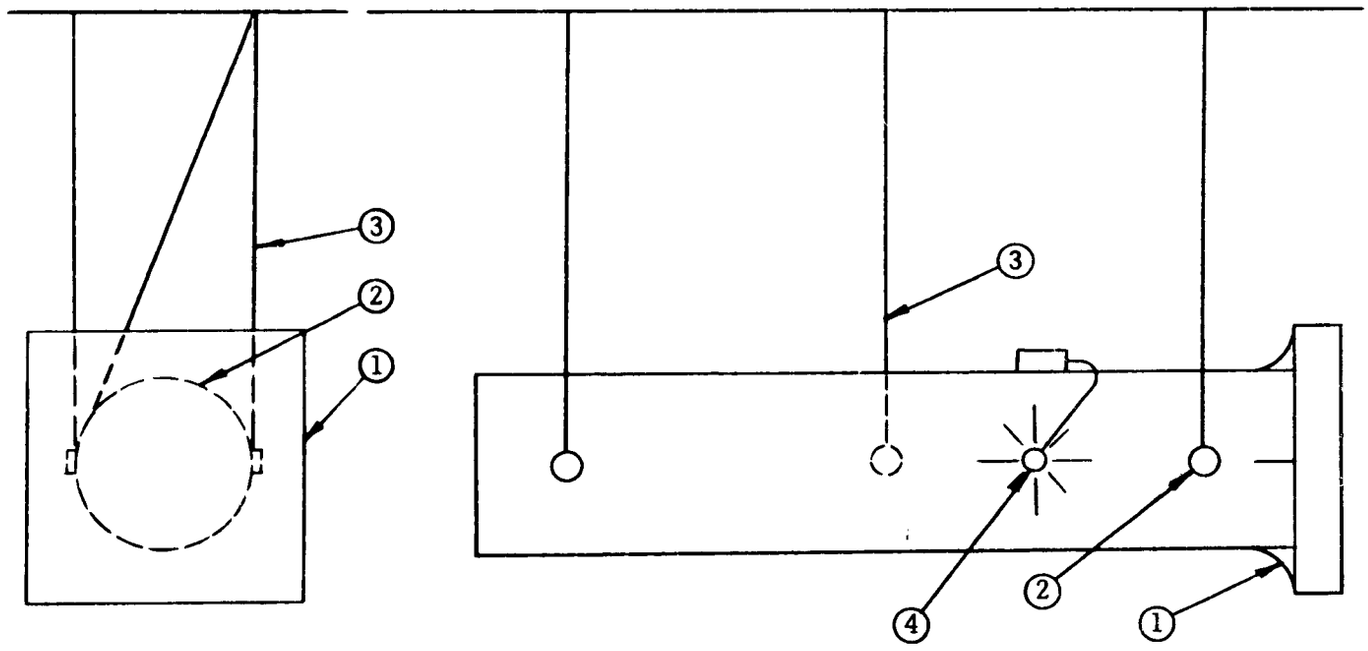

1 Target

2 Pendulum Body

3 Suspension Wires

4 Fiducial Light

Figure 28

Ballistic Pendulum

9.5.4 Data

Four shots were made with the pendulum in position and the target in place. Table I shows the data from these shots and the calculated momentum of the backspall (M_s).

Table I

Shot #	M	d	v	mv	5.33 Md	Ms
Q 350	30.44 Kg	27.5 mm	4.65 Km/sec	3.72×10^{-4}	44.62×10^{-4}	40.90×10^{-4}
Q 351	28.77 Kg	19 .5 mm	4.1 Km/sec	3.28×10^{-4}	29.9×10^{-4}	26.62×10^{-4}
Q 353	28.77 Kg	33.0 mm	3.36 Km/sec	2.69×10^{-4}	50.60×10^{-4}	47.9×10^{-4}
Q 354	33.90 Kg	31.0 mm	3.03 Km/sec	2.42×10^{-4}	56.01×10^{-4}	53.59×10^{-4}

Comparing column v with column Ms or comparing the impacting velocity with the momentum of the backspall, it is seen that the M_s does not behave as would be expected at all. To help explain this abnormal behavior, two more shots were made using the same experimented setup except the gun was intentionally aimed so the projectile would hit a baffle which was inserted in front of the pendulum. The results of those shots are tabulated in Table II.

Table II

Shot #	M	d	Velocity of Pellet at Impact on Baffle
Q 356	33.9 Kg	10 mm	4.45 Km/sec
Q 357	33.9 Kg	9 mm	4.22 Km/sec

It is evident from Table II that the muzzle blast from the light-gas gun is interfering with the experiment. The range presently used for the light-gas gun is obviously not satisfactory. The other range has the necessary baffles to eliminate the muzzle blast, but the remainder of the range would have to be modified to accomodate the pendulum. This has not been done.

9.6 Results and Recommendations

The results of the shooting in this redirection of effort have been encouraging in that they show the method of obtaining the total momentum of the backspall by difference to be a workable method. The major difficulty, that of eliminating the muzzle blast from the experiment was shown and the way to "clean up" the shot was decided upon.

The experiment to determine the temperature of the impact flash was designed and some of the possible difficulties were pointed out.

The backspall investigation should be completed. The information is necessary and apparently directly obtainable. Some modification of the second vacuum range to accomodate the pendulum is the only major obstacle to the completion of this work.

The problem of getting the temperature of the light within the crater is a little more difficult. The light of the impact, as already pointed out, is almost exclusively associated with the spray particles. The light, too, is principly atomic in origin. There is very little meaning to the temperature of the black body in this situation. A more meaningful study would be to investigate the light in the trails of the spray particles. These particles in interaction with the atmosphere have many of the characteristics of natural meteors. It is possible that information could be obtained from these artificial meteors which would solve the problems of the natural particles.

BIBLIOGRAPHY

1. Öpik, Ernest J., "Physics of Meteor Flight in the Atmosphere," Interscience Tracts on Physics and Astronomy Number 6, Interscience Publishers, Inc. (1958).

2. _____. Personal interview with Dr. E. P. Palmer and students at the University of Utah High Velocity Laboratory.

3. Bjork, Rand Corporation, Report P 1662 (1959).

4. APGC, Eglin Air Force Base, Florida, Report No. APGC-TDR-62-11, "Study of Target Penetration Prediction by High Speed and Ultra High Speed Ballistic Impact." Quarterly Report Number 2, February, 1962.

5. APGC, Eglin AFB, Florida, Report No. APGC-TDR-62-20, "Theory of High Speed Impact." Final Report, March 1962.

6. Johnson, D. K.; Cannon, E. T.; Palmer, E. P.; and Grow, R. W., "Cratering Produced in Metals by High Velocity Impact," Tech Report UU-4, Contract No. AF 04(647)-176, July 31, 1959, High Velocity Laboratory, University of Utah.

7. Kineke, "An Experimental Study of Crater Formation in Metallic Targets," Proceedings of Fourth Hypervelocity Impact Symposium, APGC-TR-60-39 (1).

INITIAL DISTRIBUTION

2	Wpns Sys Eval Gp
1	Hq USAF (AFTAC)
1	Hq USAF (AFCIN-3K2)
2	Hq USAF (AFRDC)
1	Hq USAF (AFRAE-E)
1	Hq USAF (AFTST-EL/CS)
1	Hq USAF (AFRST-PM/ME)
1	AFSC (SCRWA)
1	AFSC (SCTA)
2	BSD (AFSC)
1	ASD (ASAPRL)
1	ASD (ASRMDS)
3	ASD (ASAD-Lib)
1	ASD (ASRNGW)
2	SSD
1	OOAMA (OOYD)
2	AFSWC (Tech Info Div)
1	AFCRL (CRQST-2)
2	AFOSR
3	AFOSR (SRHP)
1	AFOSR (Univ of Utah)
1	TAC (TPL-RQD-M)
2	ARO (Scientific Info Br)
2	OAR (RROSA)
1	White Sands Msl Range (ORDBS-OM-W)
3	AMC (MCR)
2	Picatinny Arsenal (ORDBB-TK)
4	Aberdeen Proving Ground
1	Redstone Scientific Info Ctr
1	Frankford Arsenal (Lib)
1	Frankford (Pitman-Dunn Lab)
2	Springfield Armory (R&D Div)
2	Watervliet Arsenal (ORDBR-R)
2	Watertown Arsenal
1	Rock Island Arsenal
1	Engr Rsch & Dev Lab (Tech Support Br)
1	USCONARC (Special Wpns Div)
2	U.S. Army Rsch Office
4	Bu of Nav Wpns (R-12)
4	Bu of Nav Wpns (RM)
1	Nav Rsch Lab
2	Nav Ordnance Test Station
2	Nav Ordnance Test Station (Tech Lib)
2	Nav Ordnance Lab (Tech Lib)
2	Nav Wpns Lab (Tech Lib)
1	USAF Proj RAND
1	NASA
4	NASA (Langley Rsch Ctr)
4	NASA (Ames Rsch Ctr)
1	Marshall Space Flight Ctr (M-AERO-TS)
1	Marshall Space Flight Ctr (Advanced Rsch Proj Lab)
1	Advanced Rsch Proj Agcy
1	Defense Rsch & Engineering (Tech Lib)
2	Defense Rsch and Engineering
1	Armour Rsch Foundation (Def Rsch)
3	Lewis Rsch Ctr
1	Univ of Chicago (Institute for Air Wpns)
2	The Franklin Institute of the State of Penn (Tech Lib)
1	Calif Institute of Technology (Jet Propulsion Lab)
2	Johns Hopkins University (Applied Rsch Lab)
30	ASTIA (TIPCR)
	APGC
2	ASQR
9	PGAPI
3	PGEH
2	PGWR
20	PGWRT
2	PGW

Air Proving Ground Center, Eglin Air Force Base, Florida
Rpt No. APGC-TDR-62-69. TERMINAL BALLISTIC INVESTIGATION OF THE IMPACT AND EFFECT OF ULTRA HIGH SPEED MICRON-SIZE PARTICLES PRODUCED ON HYPERVELOCITY IMPACT. Final report, November 1962, 71p. incl. illus., bibliography UNCLASSIFIED REPORT

This TDR reports the results of the investigations of spray particle impact. A method was devised to measure the velocity and calculate the diameter of the spray particle in flight. The crater produced at impact was measured to obtain the diameter and several attempts to measure penetration and volume are described. A scaling law relating macro size craters to micro craters produced at the same velocity is presented.

1. Terminal ballistics
2. Particles
3. Impact
4. Hypervelocity guns
5. Hypervelocity projectiles
I. AFSC Project 5841
II. Contract AF 08(635)-2099
III. Utah Research and Development Company, Salt Lake City, Utah
IV. In ASTIA collection

Air Proving Ground Center, Eglin Air Force Base, Florida
Rpt No. APGC-TDR-62-69. TERMINAL BALLISTIC INVESTIGATION OF THE IMPACT AND EFFECT OF ULTRA HIGH SPEED MICRON-SIZE PARTICLES PRODUCED ON HYPERVELOCITY IMPACT. Final report, November 1962, 71p. incl. illus., bibliography UNCLASSIFIED REPORT

This TDR reports the results of the investigations of spray particle impact. A method was devised to measure the velocity and calculate the diameter of the spray particle in flight. The crater produced at impact was measured to obtain the diameter and several attempts to measure penetration and volume are described. A scaling law relating macro size craters to micro craters produced at the same velocity is presented.

1. Terminal ballistics
2. Particles
3. Impact
4. Hypervelocity guns
5. Hypervelocity projectiles
I. AFSC Project 5841
II. Contract AF 08(635)-2099
III. Utah Research and Development Company, Salt Lake City, Utah
IV. In ASTIA collection

Air Proving Ground Center, Eglin Air Force Base, Florida
Rpt No. APGC-TDR-62-69. TERMINAL BALLISTIC INVESTIGATION OF THE IMPACT AND EFFECT OF ULTRA HIGH SPEED MICRON-SIZE PARTICLES PRODUCED ON HYPERVELOCITY IMPACT. Final report, November 1962, 71p. incl. illus., bibliography UNCLASSIFIED REPORT

This TDR reports the results of the investigations of spray particle impact. A method was devised to measure the velocity and calculate the diameter of the spray particle in flight. The crater produced at impact was measured to obtain the diameter and several attempts to measure penetration and volume are described. A scaling law relating macro size craters to micro craters produced at the same velocity is presented.

1. Terminal ballistics
2. Particles
3. Impact
4. Hypervelocity guns
5. Hypervelocity projectiles
I. AFSC Project 5841
II. Contract AF 08(635)-2099
III. Utah Research and Development Company, Salt Lake City, Utah
IV. In ASTIA collection

Air Proving Ground Center, Eglin Air Force Base, Florida
Rpt No. APGC-TDR-62-69. TERMINAL BALLISTIC INVESTIGATION OF THE IMPACT AND EFFECT OF ULTRA HIGH SPEED MICRON-SIZE PARTICLES PRODUCED ON HYPERVELOCITY IMPACT. Final report, November 1962, 71p. incl. illus., bibliography UNCLASSIFIED REPORT

This TDR reports the results of the investigations of spray particle impact. A method was devised to measure the velocity and calculate the diameter of the spray particle in flight. The crater produced at impact was measured to obtain the diameter and several attempts to measure penetration and volume are described. A scaling law relating macro size craters to micro craters produced at the same velocity is presented.

1. Terminal ballistics
2. Particles
3. Impact
4. Hypervelocity guns
5. Hypervelocity projectiles
I. AFSC Project 5841
II. Contract AF 08(635)-2099
III. Utah Research and Development Company, Salt Lake City, Utah
IV. In ASTIA collection

Air Proving Ground Center, Eglin Air Force Base, Florida
Rpt No. APGC-TDR-62-69. TERMINAL BALLISTIC INVESTIGATION OF THE IMPACT AND EFFECT OF ULTRA HIGH SPEED MICRON-SIZE PARTICLES PRODUCED ON HYPERVELOCITY IMPACT. Final report, November 1962, 71p. incl. illus., bibliography UNCLASSIFIED REPORT

This TDR reports the results of the investigations of spray particle impact. A method was devised to measure the velocity and calculate the diameter of the spray particle in flight. The crater produced at impact was measured to obtain the diameter and several attempts to measure penetration and volume are described. A scaling law relating macro size craters to micro craters produced at the same velocity is presented.

1. Terminal ballistics
2. Particles
3. Impact
4. Hypervelocity guns
5. Hypervelocity projectiles

I. AFSC Project 5841
II. Contract AF 08(635)-2099
III. Utah Research and Development Company, Salt Lake City, Utah
IV. In ASTIA collection

Air Proving Ground Center, Eglin Air Force Base, Florida
Rpt No. APGC-TDR-62-69. TERMINAL BALLISTIC INVESTIGATION OF THE IMPACT AND EFFECT OF ULTRA HIGH SPEED MICRON-SIZE PARTICLES PRODUCED ON HYPERVELOCITY IMPACT. Final report, November 1962, 71p. incl. illus., bibliography UNCLASSIFIED REPORT

This TDR reports the results of the investigations of spray particle impact. A method was devised to measure the velocity and calculate the diameter of the spray particle in flight. The crater produced at impact was measured to obtain the diameter and several attempts to measure penetration and volume are described. A scaling law relating macro size craters to micro craters produced at the same velocity is presented.

1. Terminal ballistics
2. Particles
3. Impact
4. Hypervelocity guns
5. Hypervelocity projectiles

I. AFSC Project 5841
II. Contract AF 08(635)-2099
III. Utah Research and Development Company, Salt Lake City, Utah
IV. In ASTIA collection

Air Proving Ground Center, Eglin Air Force Base, Florida
Rpt No. APGC-TDR-62-69. TERMINAL BALLISTIC INVESTIGATION OF THE IMPACT AND EFFECT OF ULTRA HIGH SPEED MICRON-SIZE PARTICLES PRODUCED ON HYPERVELOCITY IMPACT. Final report, November 1962, 71p. incl. illus., bibliography UNCLASSIFIED REPORT

This TDR reports the results of the investigations of spray particle impact. A method was devised to measure the velocity and calculate the diameter of the spray particle in flight. The crater produced at impact was measured to obtain the diameter and several attempts to measure penetration and volume are described. A scaling law relating macro size craters to micro craters produced at the same velocity is presented.

1. Terminal ballistics
2. Particles
3. Impact
4. Hypervelocity guns
5. Hypervelocity projectiles

I. AFSC Project 5841
II. Contract AF 08(635)-2099
III. Utah Research and Development Company, Salt Lake City, Utah
IV. In ASTIA collection

Air Proving Ground Center, Eglin Air Force Base, Florida
Rpt No. APGC-TDR-62-69. TERMINAL BALLISTIC INVESTIGATION OF THE IMPACT AND EFFECT OF ULTRA HIGH SPEED MICRON-SIZE PARTICLES PRODUCED ON HYPERVELOCITY IMPACT. Final report, November 1962, 71p. incl. illus., bibliography UNCLASSIFIED REPORT

This TDR reports the results of the investigations of spray particle impact. A method was devised to measure the velocity and calculate the diameter of the spray particle in flight. The crater produced at impact was measured to obtain the diameter and several attempts to measure penetration and volume are described. A scaling law relating macro size craters to micro craters produced at the same velocity is presented.

1. Terminal ballistics
2. Particles
3. Impact
4. Hypervelocity guns
5. Hypervelocity projectiles

I. AFSC Project 5841
II. Contract AF 08(635)-2099
III. Utah Research and Development Company, Salt Lake City, Utah
IV. In ASTIA collection